Vitreous Changes in Myopia

11

Shoji Kishi

11.1 Introduction

The vitreous has a transparent gel-like structure with 4 ml of volume. The vitreous gel is covered by the vitreous cortex which consists of densely packed collagen. The Cloquet's canal arises from Martegiani space at the optic disc and traverses the central vitreous to retrolental space known as Berger's space. Although the vitreous appears inert, it plays a major role in various fundus diseases including rhegmatogenous retinal detachment, macular hole, epiretinal membrane, and progression of proliferative diabetic retinopathy. Recently vitreous surgery expands its indication in vitreoretinal diseases such as diabetic macular edema and myopic foveoschisis [1, 2]. The vitreous is not a homogeneous tissue which is the subject for resection in vitrectomy. The vitreous has its own structure which has been elucidated by biomicroscopy of postmortem eyes. Recent advance of optical coherent tomography greatly improved our understanding on vitreous anatomy and vitreoretinal interface diseases.

In myopic eyes, vitreous liquefaction develops at an early age which results in earlier posterior vitreous detachment (PVD). There is a strong statistical relation between axial myopia and rhegmatogenous retinal detachment [3]. Vitreous surgeons frequently encounter a membranous structure on the retina in eyes with myopic foveoschisis despite the apparent PVD with Weiss ring. In this chapter, the vitreous anatomy and its age-related change are described in normal eyes as well as vitreous changes in myopic eyes.

S. Kishi, MD
Department of Ophthalmology,
Gunma University School of Medicine,
Gunma University Hospital, 3-39-15 Showamachi,
Maebashi, Gunma 371-8511, Japan
e-mail: kishi@med.gunma-u.ac.jp

11.2 Anatomy of the Vitreous

11.2.1 Embryology of the Vitreous [4]

11.2.1.1 Formation of Primary Vitreous (Fourth to Sixth Week; 4–13 mm Stage)

The primary vitreous first appears in the narrow space between the surface and neural ectoderm during the fourth week of gestation, when the embryo is 4–5 mm in length. It derived mostly from the surface and neural ectoderm and partly from the mesoderm invaded through the embryonic choroidal fissure. The condensed fibrils of the primary vitreous form the *capsula perilenticularis fibrosa* around the lens. At the 5–7 mm stage, the hyaloid artery enters the distal part of optic stalk through the fetal fissure. It reaches the *capsula perilenticularis fibrosa* at 7 mm stage. The *capsula* is then vascularized by hyaloid artery and develops the *tunica vasculosa lentis* by the 13 mm stage.

11.2.1.2 Formation of Secondary Vitreous (Sixth Week to Third Month; 13–70 mm Stage)

The secondary vitreous is the major component of the adult vitreous body which is derived from the neural ectoderm. At the end of the sixth week or 13 mm stage, the secondary vitreous emerges between the developing retina and the primary vitreous. It grows around the primary vitreous and crowds it axially. An intravitreous limiting membrane develops as a condensation layer between the primary and secondary vitreous; it becomes the wall of Cloquet's canal. By the third month, the secondary vitreous fills two-thirds of the volume of the optic cup. After the 16 mm stage, hyaloid artery forms the *vasa hyaloidea propria*, which reaches maximum at the 40–60 mm stage. During the second month to the fifth month, a cone-shaped cellular mass called Bergmeister's papilla develops. Lens *zonule of Zinn* develops during 70–110 mm stage.

R.F. Spaide et al. (eds.), *Pathologic Myopia*,
DOI 10.1007/978-1-4614-8338-0_11,

11.2.1.3 Late Fetal Development

During the fourth to ninth month, or between the 110 and 300 mm stage, the globe undergoes rapid growth. The vitreous body enlarges as a result of growth of the secondary vitreous. Hyaloid vascular system atrophies leaving a few filamentous structures in Cloquet's canal. Between the 110 and 150 mm stage, or during the fifth month, the *tunica vasculosa lentis* regresses.

11.2.2 Vitreous Development After Birth

At birth, vitreous gel appears homogeneous with no liquefaction. Cloquet's canal runs a straight course from the lens to the optic disc. Thereafter, it sags until its superior portion hangs behind the posterior lens surface. The vitreous gel shows pattern of radial fibers at new born. At adolescent, lamellar structure which is called "tractus vitreales" is formed in anterior part of the vitreous [5]. Tractus vitreales traverse the whole vitreous in adult. In the macular area, early sign of vitreous liquefaction is seen at new born [6]. "Posterior precortical vitreous pocket" [7] develops by the age of 5 years.

11.2.3 Microscopic Anatomy

11.2.3.1 The Vitreous Body

The vitreous consists of 98 % water and 2 % protein which include collagen, hyaluronan, chondroitin sulfate, and other non-collagenous proteins. Collagen builds up three-dimensional meshwork of the vitreous gel. Type II collagen comprises 75 % of the total collagen content [8], and type IX accounts for 15 % [9]. Hyaluronan is a large polyanion which entangles to the vitreous collagen fibrils and attracts a large amount of water in the vitreous gel. The vitreous base is a circumferential zone with 2–6 mm width from peripheral retina to pars plana of the ciliary body. Vitreous fibers splay out from the vitreous base to the ciliary body, central vitreous, and posterior pole. The vitreous cortex is a shell of the vitreous gel which has higher density of collagen than inner vitreous. The vitreous cortex is 100–200 um thick. Hyalocytes are embedded in the vitreous cortex with highest density in the vitreous base followed by the posterior pole. Its role in metabolism is controversial. Hyalocytes appear to act as tissue macrophage [10]. The anterior vitreous cortex attaches to the posterior lens capsule in a circular zone about 8 mm in diameter (Weiger's ligament).

11.2.4 Vitreoretinal Interface

In the outermost layer of the vitreous cortex, vitreous collagen merges with the internal limiting membrane (ILM) of the retina and the basement membrane of the ciliary epithelium. The ILM consists of type IV collagen, associated with glycoprotein, type VI collagen which may contribute to vitreoretinal adhesion, and type XVIII, which binds opticin. Opticin binds to heparin sulfate, contributing to vitreoretinal adhesion [11]. The posterior vitreous cortex has lamellar structure [12], which may attribute the splitting of vitreous cortex in partial vitreous detachment. The strength of vitreous attachment to the surrounding tissue differs on the location. The vitreous base has the firmest attachment. The vitreous collagen fibrils are radial oriented and inserted in the basement membrane or cell processes of adjacent retinal and ciliary epithelial cells in the vitreous base. A second firm area of attachment is along the peripheral margin of the optic nerve head. The relatively firm vitreoretinal attachment is present at the margin and the center of the fovea, which cause perifoveal vitreous detachment. Vitreoretinal adhesion is occasionally observed along the retinal vessels. The ILM is the basement membrane of Müller cells. The ILM is uniformly thin (51 nm) within the vitreous base, but progressively and irregularly thickened in the equatorial zone (sixfold) and posterior zone (37-fold) [13]. The ILM is extremely thin at vitreous base, optic disc, and fovea. The ILM is also very thin over major retinal vessels where defect allows glial cells to extend on to the inner retina [14]. The location of firm vitreoretinal attachment corresponds to the area of thinner ILM.

11.2.5 Biomicroscopic Anatomy

The anatomy of the vitreous has been studied using dark-field slit microscopy on postmortem eyes by carefully separating the sclera, choroid, and retina from the vitreous and immersed in physiological solution to preserve its three-dimensional structure. Eisner [5] observed vitreous veils which he labeled *tracts hyaloideus* (inner wall of Cloquet's canal), *tractus coronarius, tractus medianus, and tractus preretinalis*. These vitreous veils are not observed in newborn but only developed in adult (Fig. 11.1).

Worst studied the vitreous by selective colored India ink injection after removal of the sclera, choroid, and retina from vitreous body. He showed a cistern system in the adult eyes [15, 16] (Fig. 11.2). The cistern system comprises 72 cisterns around the vitreous core at the level of posterior margin of the ciliary body, 36 cisterns at the level of the equator, and 12 large cisterns in the posterior vitreous. The central posterior vitreous consists of the *cistern preoptica* (prepapillary area of Martegiani), the *bursa premacularis*, and the *circumpapillo-macular cisterns*. The *bursa premacularis* is the posterior extension of the *canalis ciliobursale* which runs in an incomplete spiral from the ciliary body region towards the macular area. The posterior wall of the *bursa* was very thin, the fibers consisted of fine radiating lines, and there were three concentric rings at the posterior portion. The *bursa*

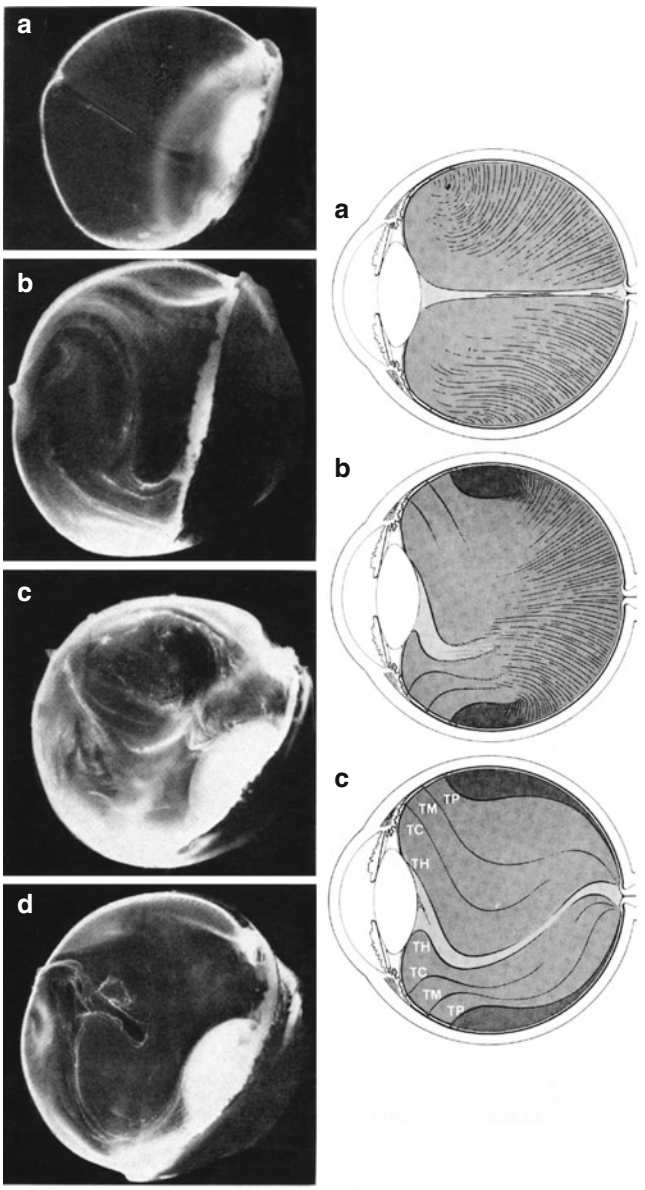

Fig. 11.1 Lamellar structure of the vitreous. *Left*: optical section through the vitreous body from the papilla towards the middle of the posterior surface of the lens. (**a**) 7-month-old child, (**b**) 40-year-old man, (**c**) 35-year-old man, (**d**) 60-year-old man. *Right*: schematic drawing of development of vitreous structure. (**a**) Newborn, (**b**) adolescent, (**c**) adult. *TC* tractus coronarius, *TH* tractus hyaloideus, *TM* tractus medianus, *TP* tractus preretinalis (Reprint from Eisner [5], p106 (*right*) and p107 (*left*))

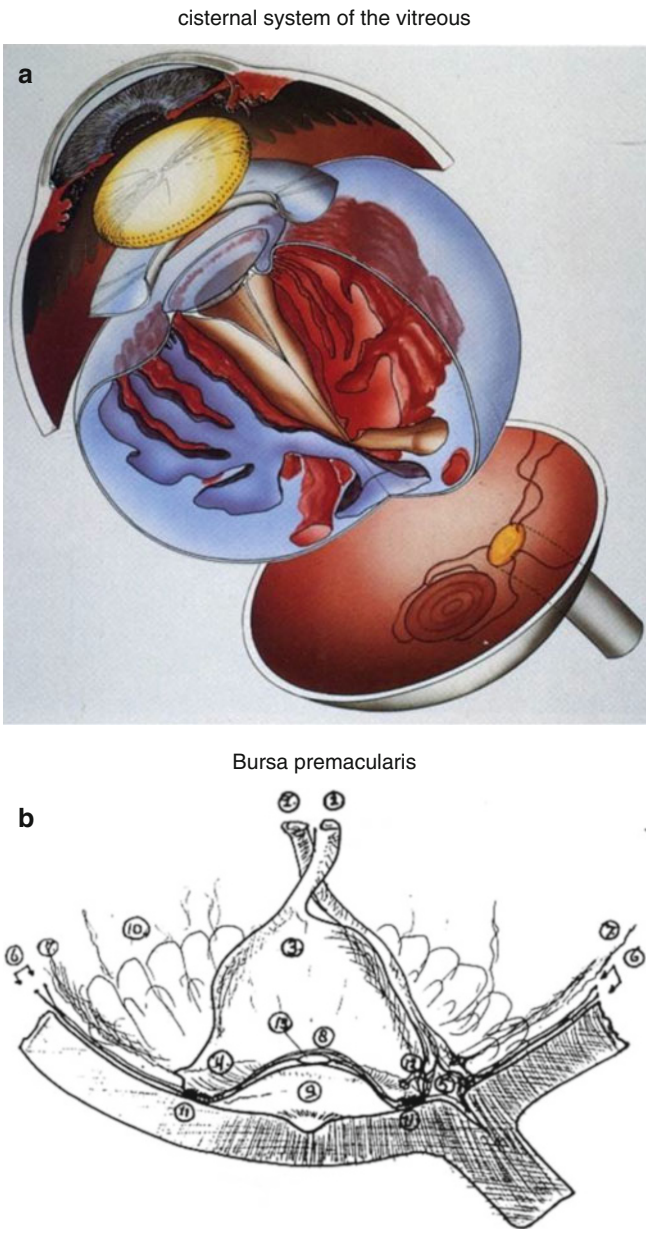

Fig. 11.2 *Top*: cisternal system of the vitreous according to worst (Reprint from Sebag [35], p163. *Bottom*: bursa premacularis. Enlarged schematic: *1* canal of Cloquet, *2* superior branching channel, *3* capula of bursa premacularis, *4* fornix of bursa, *5* area of Martegiani, *6* vitreoretinal limiting membrane (Gärtner), *7* tractus preretinalis (Eisner), *8* pars patelliformis membranae vitrealis, *9* spatium subbursale premaculare, *10* corona petaliformis, *11* perimacular bonding ring, *12* lower branching channel, *13* ocellus prefovealis (Reprint from Worst [16])

premacularis is situated on the convexly detached vitreous cortex which forms *subbursal space*. In his early publication [16], Worst stated that a separation was present between the prefoveal part of the *bursa premacularis* and the fovea, which he named the "subbursal space." This space could be viewed through the center of the base of the *bursa premacularis* named the "ocellus prefovealis." From his point of view, the posterior wall of the bursa is anatomically detached from the retina, which makes impossible the posterior wall to exert the anterior traction to the macula. In later specimens, Worst noted that this was a postmortem artifact. He revised that the posterior wall of the *bursa* is a thin vitreous cortex itself [17].

Sebag et al. [18] observed two holes in the vitreous cortex which corresponded to prepapillary hole and premacular hole. Vitreous fibers extruded posteriorly through the premacular hole (Fig. 11.3 top).

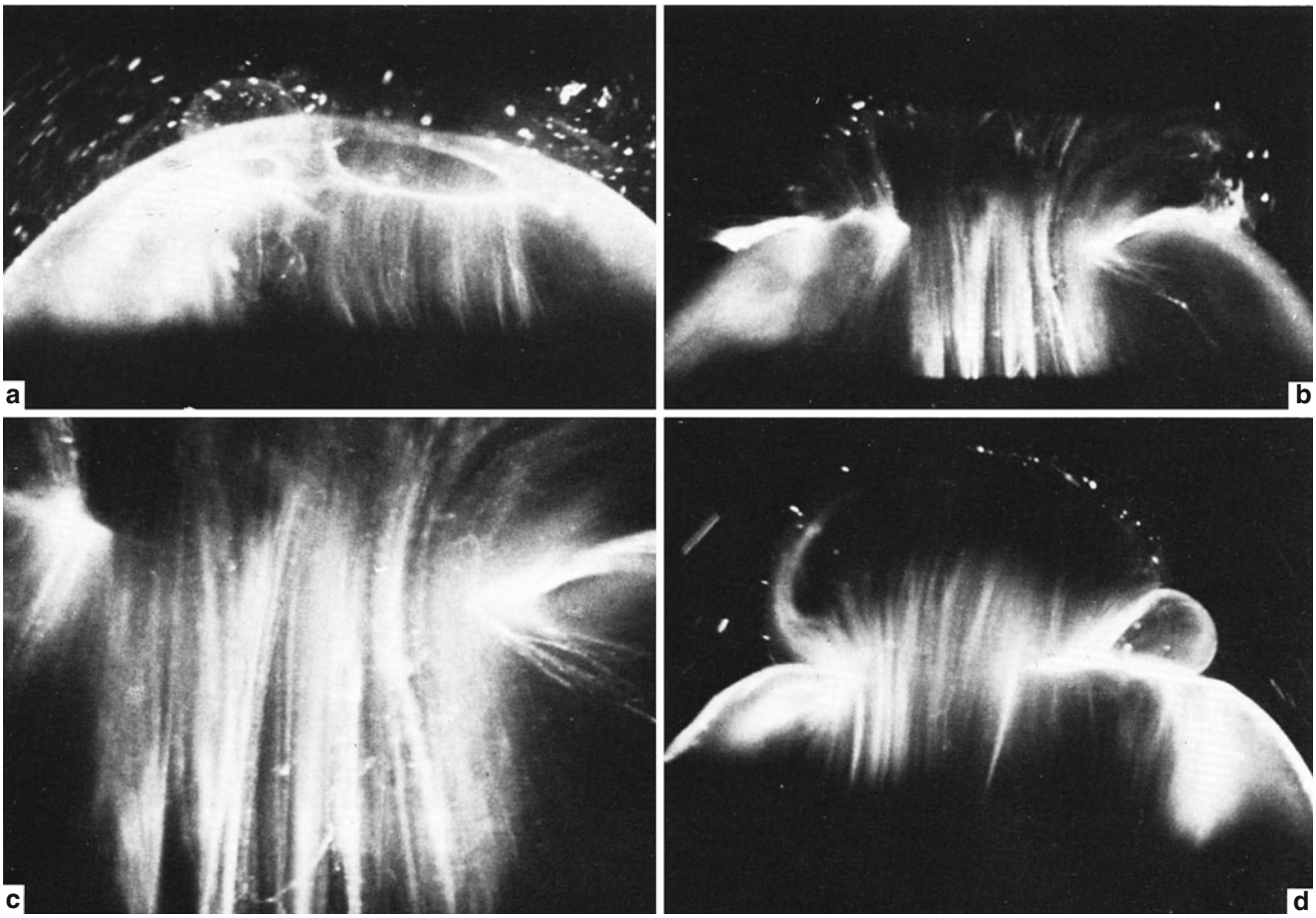

Fig. 11.3 (**a**) Posterior vitreous in the left eye of a 52-year-old male. The vitreous is enclosed by the vitreous cortex. There are two holes in the prepapillary (small, to the *left*) and premacular (large, to the *right*) vitreous cortex. Vitreous fibers are oriented toward the premacular region. (**b**) Posterior vitreous in a 57-year-old male. A large bundle of prominent fibers is seen coursing anteroposteriorly and entering the retrohyaloid space via the premacular hole in the vitreous cortex. (**c**) Same as (b) at higher magnification. (**d**) Posterior vitreous in the right eye of a 53-year-old female. There is posterior extrusion of the vitreous out the prepapillary hole (to the *right*) and premacular (large extrusion to the *left*) vitreous cortex. Fibers course anteroposteriorly out into the retrohyaloid space

11.2.6 Posterior Precortical Vitreous Pocket (PPVP)

11.2.6.1 Biomicroscopy of Posterior Precortical Vitreous Pocket

Kishi et al. studied the vitreous structure and the vitreoretinal interface (by preserving the retina in a bisected eyeball specimen) by staining its gel component with fluorescein [7]. The vitreous lacuna anterior to the posterior pole was always present in adult eyes. The posterior wall of the lacuna was a thin vitreous cortex, and the anterior extent was delineated by vitreous gel (Fig. 11.4). This physiological vitreous lacuna was defined as "posterior precortical vitreous pocket" (PPVP). This is seemingly the same structure as observed by Worst (*bursa permacularis*) [16], but has been defined differently. The presence of PPVP denies the conventional concept of vitreomacular traction where it was believed that anteroposteriorly oriented vitreous fiber exerts the direct traction to the fovea. Because vitreous gel and posterior vitreous cortex is separated by PPVP, the vitreous traction to fovea should be transmitted through the posterior vitreous cortex. Unlikely to the definition of *bursa premacularis*, PPVP is not a sack with its outer membrane but a liquefied space. The posterior wall of PPVP is the posterior vitreous cortex attached to the retina. There is no subbursal space between the bursa and the retina. While its posterior wall of PPVP is a thin vitreous cortex itself, the anterior border is a vitreous gel. The anterior extent of the PPVP becomes larger and ill defined in the eyes with vitreous liquefaction. It is difficult to observe the entire structure of transparent PPVP by slit-lamp biomicroscopy in living eyes. Triamcinolone-assisted vitreous surgery clearly demonstrates the PPVP [19].

11.2.6.2 Optical Coherence Tomography of Posterior Precortical Vitreous Pocket

Spectral domain optical coherence tomography (SD-OCT) and its noise-reduced version enabled the first visualizations

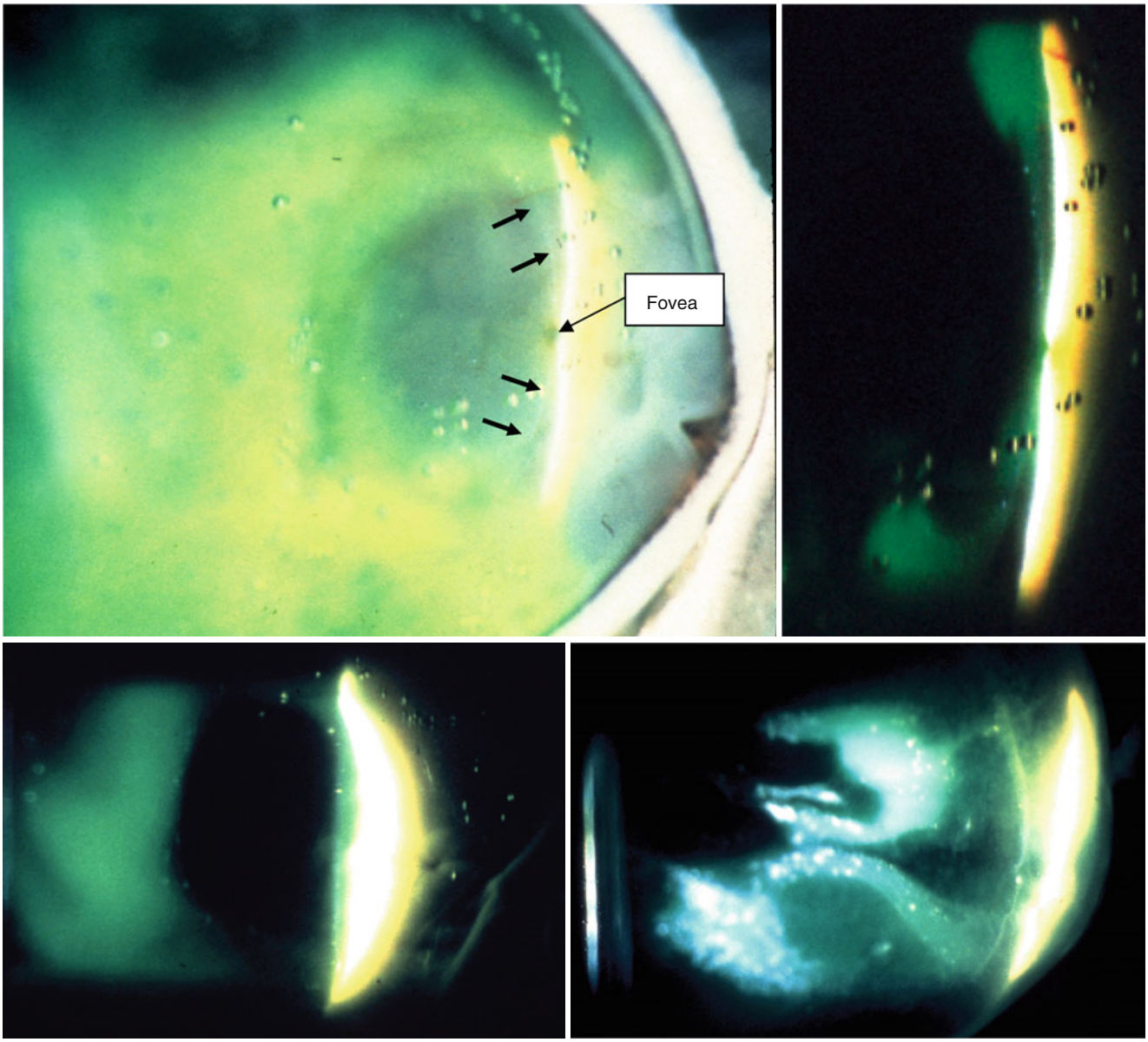

Fig. 11.4 Posterior precortical vitreous pocket (PPVP). *Top*: (*left*) bisected senile eye with background illumination. *Arrows* indicate the posterior wall of the PPVP. Optical section of PPVP in the same specimen. Posterior wall of the PPVP is a thin vitreous cortex. *Bottom*: optical section of PPVP in an eye of a 28-year-old adult (*left*) with no liquefied lacuna in the inner vitreous and senile eye (*right*) with liquefied lacunae in the inner vitreous (Reproduced from Kishi and Shimizu [7])

of the PPVP in vivo [20, 21]. Recently introduced swept source OCT (SS-OCT) enabled further clear demonstration of entire structure of PPVP (Fig. 11.5). PPVP is a boat-shaped vitreous lacuna in front of the posterior pole [22]. The superior bow of the boat is elevated interiorly in sitting position. The posterior wall is a thin vitreous cortex which is thinnest at the fovea. The anterior extent of PPVP is delineated by the vitreous gel. In eyes with little liquefaction, the anterior border of PPVP is sharply demarcated. There is a septum between the Martegiani space in Cloquet's canal and PPVP. A channel over the anterior border of the septum connects the two spaces. In the vitreous gel surrounding the PPVP, a vitreous fiber is perpendicularly inserted in the vitreous cortex. The configuration of the PPVP was almost symmetrical in both eyes of each subject. Fully developed PPVP is seen even in children older than 5 years. Yokoi et al. recently reported precursor stage of PPVP in newborn babies using SS-OCT [6].

11.2.6.3 Clinical Implication of Posterior Precortical Vitreous Pocket

Pseudo PVD

Because of PPVP, vitreous gel is always separated from the retina. The vitreous cortex, which serves as a posterior wall of PPVP, is invisible on slit-lamp biomicroscopy as long as it is attached to the retina. This condition is often misdiagnosed

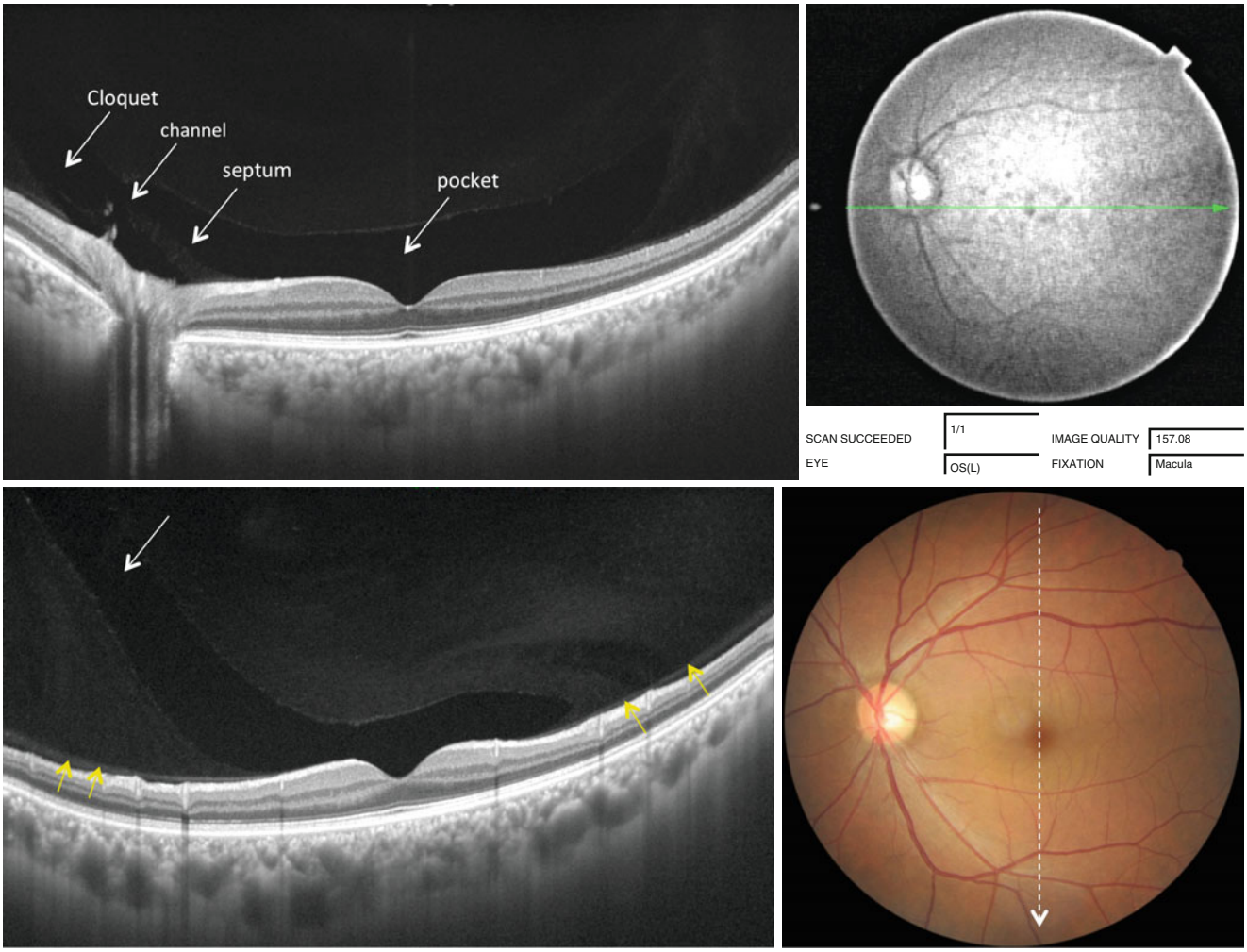

Fig. 11.5 Normal posterior precortical vitreous pocket (PPVP) with little vitreous liquefaction observed by SS-OCT. Left eye of a 46-year-old man with moderate myopia of −5.0D. *Top*: in horizontal section, PPVP is boat shaped, which is sharply demarcated by vitreous gel. There is a connecting channel between Cloquet's canal and the pocket over the septum. *Bottom*: in vertical section, superior portion of PPVP is usually elevated (*arrows*). In the vitreous gel outer to the PPVP, vitreous fiber perpendicularly inserted in the vitreous cortex

as PVD. Balazs [23] termed "vitreoschisis" to denote severe liquefaction in the posterior vitreous but persistent attachment of the outermost layer of posterior vitreous cortex on the retina. Vitreoschisis can be interpreted as a large PPVP which often develops in axial myopia.

Perifoveal PVD

The posterior wall of the PPVP exists as a membrane separated from the gel. The premacular cortex is spared from direct traction of vitreous gel but tends to develop trampoline-like detachment. However, there is a strong attachment at the fovea, which modifies the trampoline PVD to perifoveal PVD. In perifoveal PVD, the vitreous cortex is inwardly detached in the perifoveal area, which suggests elastic nature of premacular cortex. Persistent vitreous traction by perifoveal PVD may cause macular hole [24, 25] or vitreomacular traction syndrome. Perifoveal PVD physiologically occurs in the precursor stage of complete PVD [26, 27] (Fig. 11.6).

Residual Vitreous Cortex

Because the premacular vitreous cortex is separated from the gel before initiation of PVD, it occasionally remains attached to the retina during PVD [28]. The residual cortex becomes the main source of epiretinal membrane. In eyes with ERM, oval defect of premacular hyaloid is often observed in detached posterior hyaloid [29].

Diabetic Retinopathy

In diabetic retinopathy, fibrovascular proliferation tends to develop around the PPVP which results in ring-shaped fibrovascular proliferation [30]. Vitreous detachment tends to occur outer to the PPVP, but not in the area of PPVP. Outer to the PPVP, vitreous fibers insert into the vitreous cortex thus the gel and the cortex detach together. However, premacular vitreous cortex is spared from direct traction of vitreous gel because of PPVP. The posterior wall of the pocket develops trampoline-like

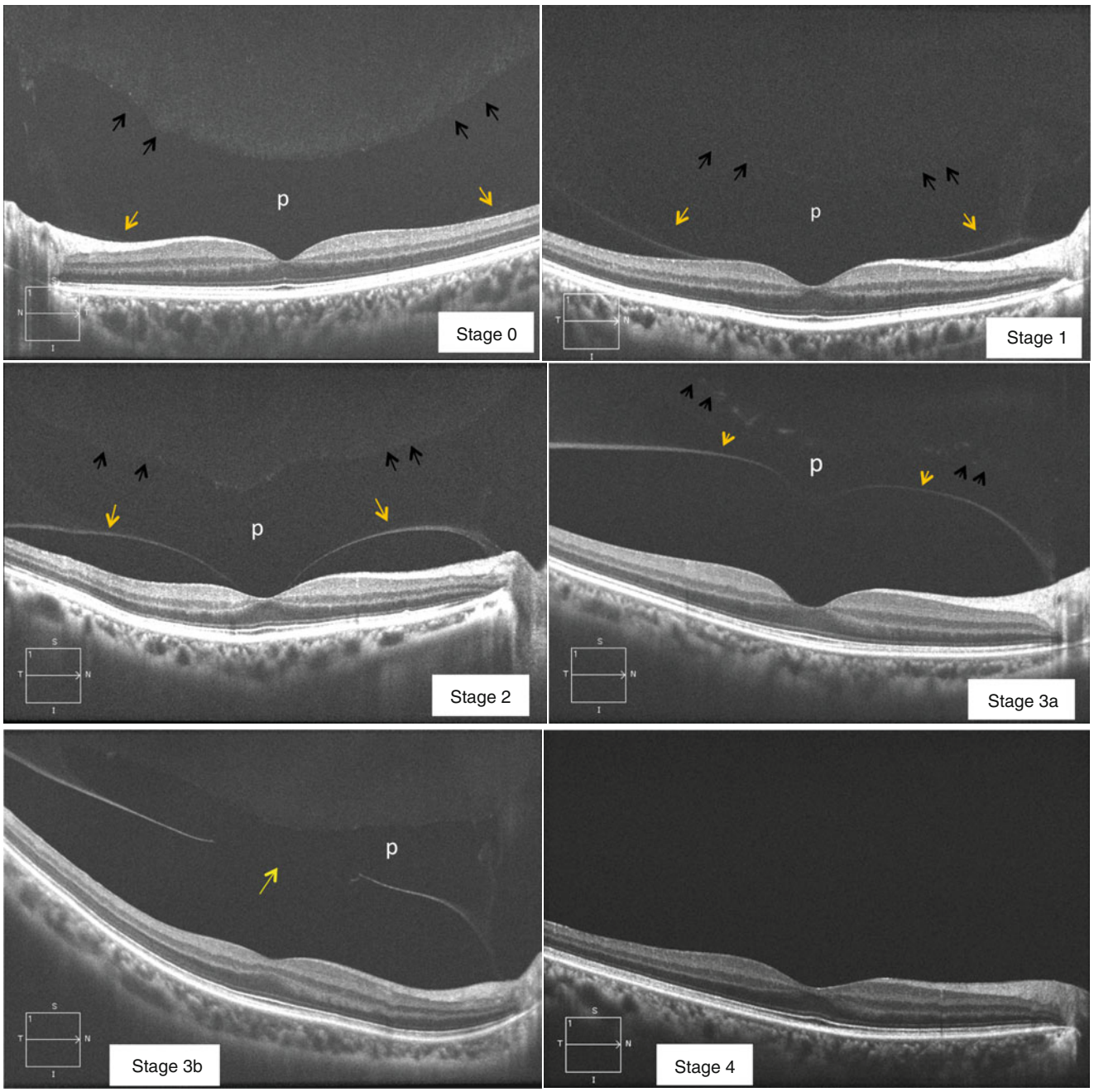

Fig. 11.6 *Top left*: Stage 0: no PVD. Posterior precortical vitreous pocket (PPVP) (p) is present anterior to the macula. Posterior wall of the PPVP is thin vitreous cortex (*yellow arrows*) and anterior border is vitreous gel (*black arrows*). *Top right*: Stage 1: Vitreous cortex is detached in paramacular area (*yellow arrows*). *Black arrows* are the anterior border of the PPVP (p). *Middle left*: Stage 2: Perifoveal PVD (*yellow arrows*). *Black arrows* indicate the anterior border of the PPVP (p). *Middle right*: Stage 3a: Macular PVD with intact vitreous cortex or the posterior wall (*yellow arrows*) of the PPVP (p). *Black arrows* indicate the anterior border of the PPVP. *Bottom left*: Stage 3b: Macular PVD with disrupted posterior wall (*yellow arrow*) of the PPVP (p). *Bottom right*: Stage 4: Complete PVD with Weiss ring. No vitreous structure is observed

PVD or perifoveal PVD which may cause cystoids macular edema [31].

Vitreoretinal Adhesion at the Fovea

Kishi et al. examined 59 human autopsy eyes with complete PVD by scanning electron microscope [28]. They found vitreous cortex remnants at the fovea in 26 out of 58 (44 %) eyes. One half of the 26 eyes had 500 μ diameter disc of remnant cortex at the fovea, which was occasionally surrounded by another 1,500 μ diameter ring of remnant cortex (Fig. 11.7a top). A 500 μ diameter ring of cortical remnant was adherent to the outer margin of the fovea in 30 % of the eyes (Fig. 11.7b left bottom). Twenty percent of the eyes showed a pseudocyst formation where a 200–300 μ diameter

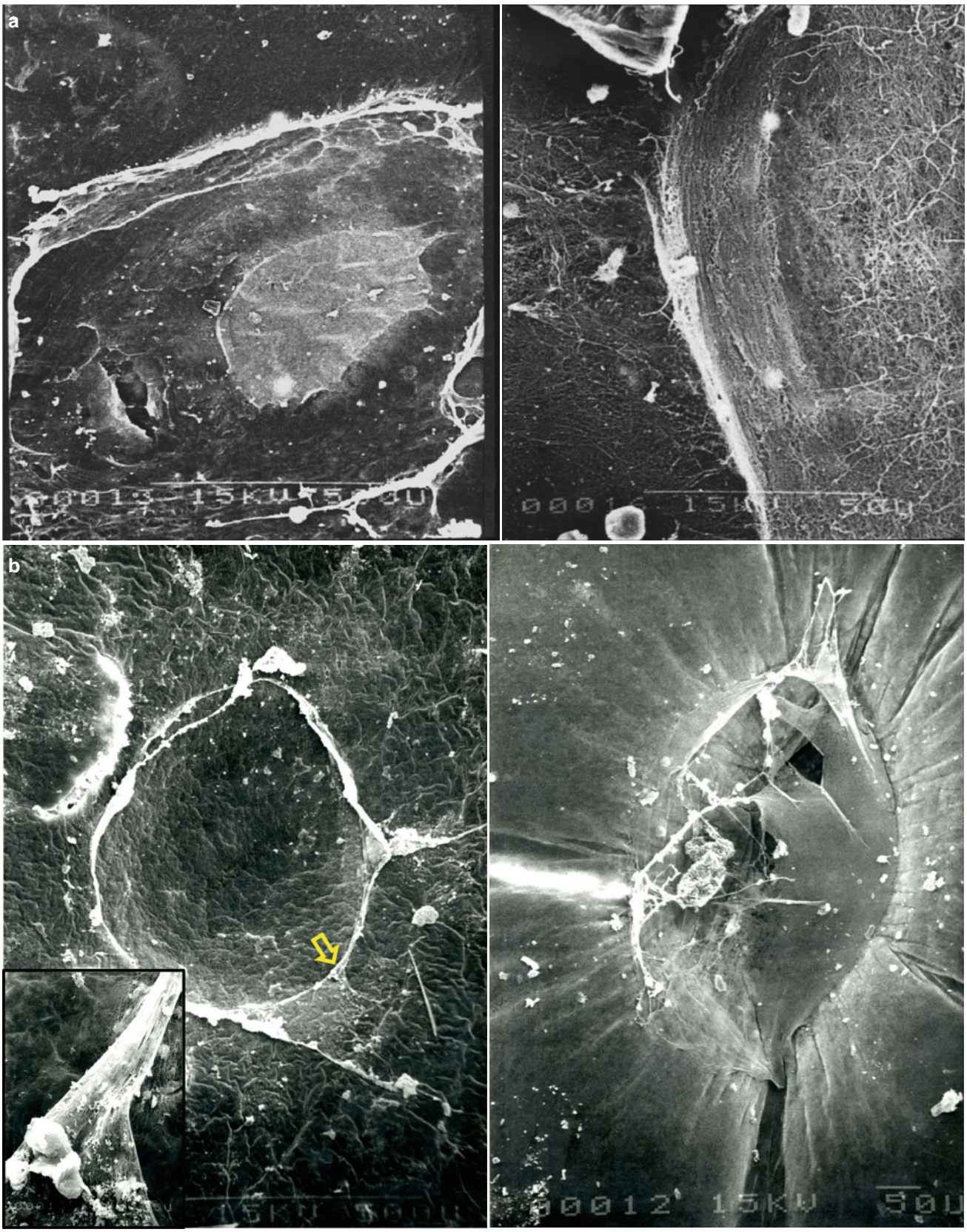

Fig. 11.7 Scanning electron microscopy of vitreous cortex remnant at the fovea (Reproduced from Kishi et al. [28]). *Top*: (*left*) 500 μ diameter disc of remnant cortex at the fovea, which was surrounded by another 1,500 μ diameter ring of remnant cortex. (*Right*) high magnification of residual vitreous cortex. *Bottom*: (*left*) ring-shaped remnant at the outer margin of foveal pit. *Inset* shows high magnification of the site of yellow arrow. (*Right*) vitreous cortex bridging the foveal pit

disc of vitreous cortex bridged over the foveal pit (Fig. 11.7b right bottom). These findings suggest strong adhesion of vitreous cortex at the fovea and the outer margin of the foveal pit. These cortical remnants were membranes with no overlying vitreous gel because vitreous cortex is separated from gel by intervening PPVP. Spaide et al. observed the foveal anatomy in patients with perifoveal PVD (mainly patients with macular holes and those with early macular hole states) using OCT [32]. They reported that the diameter of the vitreous attachment in eyes with perifoveal PVD correlated with induced changes in foveal anatomy. Normal foveal depression is seen in eyes with vitreous attachment of 1,828 um diameter, whereas loss of foveal depression is seen in vitreous attachment with 840 um diameter and foveal cavitation in 281 um of vitreous attachment.

11.3 Age-Related Change of the Vitreous

11.3.1 Liquefaction

Balazs measured the volumes of vitreous liquefaction and gel in 610 human eyes [33]. Liquid vitreous appears by the age of five and increases throughout life until it constitutes more than 50 % of volume of the vitreous during the tenth decade (Fig. 11.8). Gel vitreous volume increases during the first decade while the eye is growing in size. The volume of gel vitreous remains stable till about the age of 40, when it begins to decrease in equivalent to the increase in liquid vitreous. Foos studied the relationship between synchysis (liquefaction) senilis of vitreous and posterior vitreous detachment (PVD) in 2,246 autopsied eyes using the technique of suspension in air [34]. They showed that with age, liquefaction and incidence of PVD increases. There was a significant increase in PVD associated with grade 3 (50 % destruction) and grade 4 (67 %) synchysis. Using dark-field slit illumination, Eisner [5] and Sebag [18, 35] showed age-related changes of the vitreous. The vitreous is composed of homogeneous gel with Cloquet's canal in a 7-month-old child [5]. There is no liquefied lacuna in the eyes of 4- and 8-year-old children. Vitreous extruded into retrohyaloid space through the premacular vitreous cortex. There is no liquefaction or fibers in the vitreous. In the eyes of a 57-year-old male, a large bundle of prominent fibers is seen coursing anteroposteriorly and entering the retrohyaloid space via the premacular hole in the vitreous cortex [35] (Fig. 11.3b bottom). In the eyes of an 88-year-old woman, the fibrous structure of the vitreous was degenerated with fibers being thickened and tortuous [35]. The entire inner vitreous undergoes dissolution with empty spaces adjacent to the thickened fibers. It is believed that dissolution of the HA-collagen complex results in the simultaneous formation of liquid vitreous and aggregation of collagen into bundle of parallel fibrils and seen as large fibers. Slit-lamp biomicroscopy shows that vitreous liquefaction is associated with aggregation of collagen fibers (Fig. 11.9). In the vitreous samples obtained during vitrectomy, vitreous hyaluronan level was significantly decreased with aging [36].

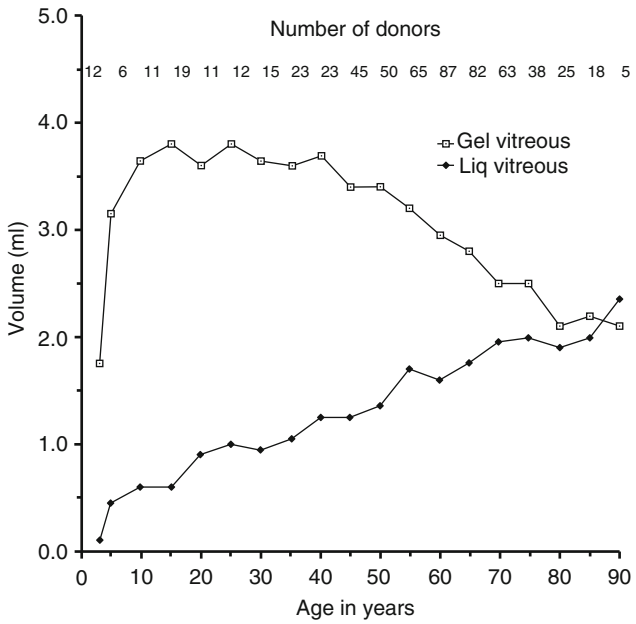

Fig. 11.8 The volumes of vitreous liquefaction and gel in 610 human eyes (Reprint from Balazs and Flood [33])

11.3.2 Posterior Vitreous Detachment (PVD)

PVD occurs when liquefied vitreous passes through a break of vitreous cortex to retrohyaloid space. Vitreous cortex detaches from internal limiting membrane of the retina during PVD. Incidence of posterior vitreous detachment (PVD) increases markedly between ages 50 and 70 years [33, 34]. As shown by Sebag in autopsy eyes, vitreous gel extrudes to retrohyaloid space through premacular hole in living eyes (Fig. 11.10). Premacular hole seems to correspond to the defect or break of the posterior wall of the PPVP. Since vitreoretinal adhesion is strongest at the optic nerve head, presence of prepapillary ring called Weiss ring in the detached vitreous cortex signifies completion of PVD (Fig. 11.11).

11.3.3 Evolution of Vitreomacular Detachment

PVD had been believed to be an acute event. However, OCT has revealed a precursor stage of complete PVD [26, 27]. Because of PPVP, the premacular vitreous cortex is spared from direct traction of the vitreous gel. Premacular

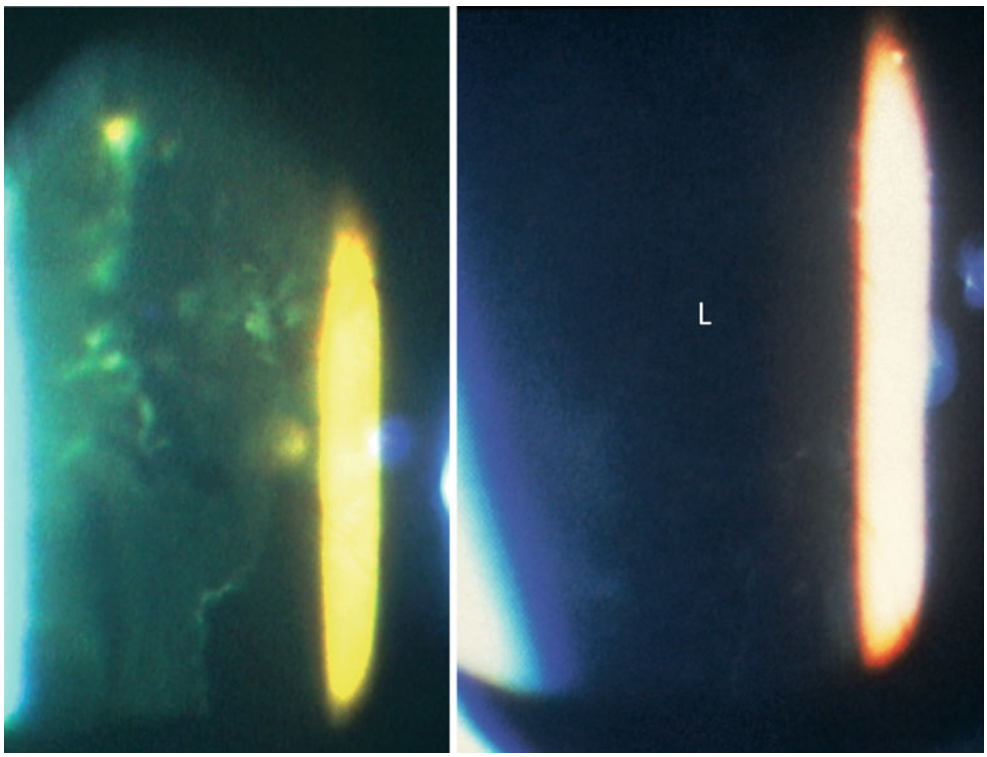

Fig. 11.9 Vitreous liquefaction in slit-lamp biomicroscopy. (*Left*) non-myopic eye with posterior vitreous detachment (PVD). (*Right*) myopic eye with large lacuna (*L*) which mimics PVD

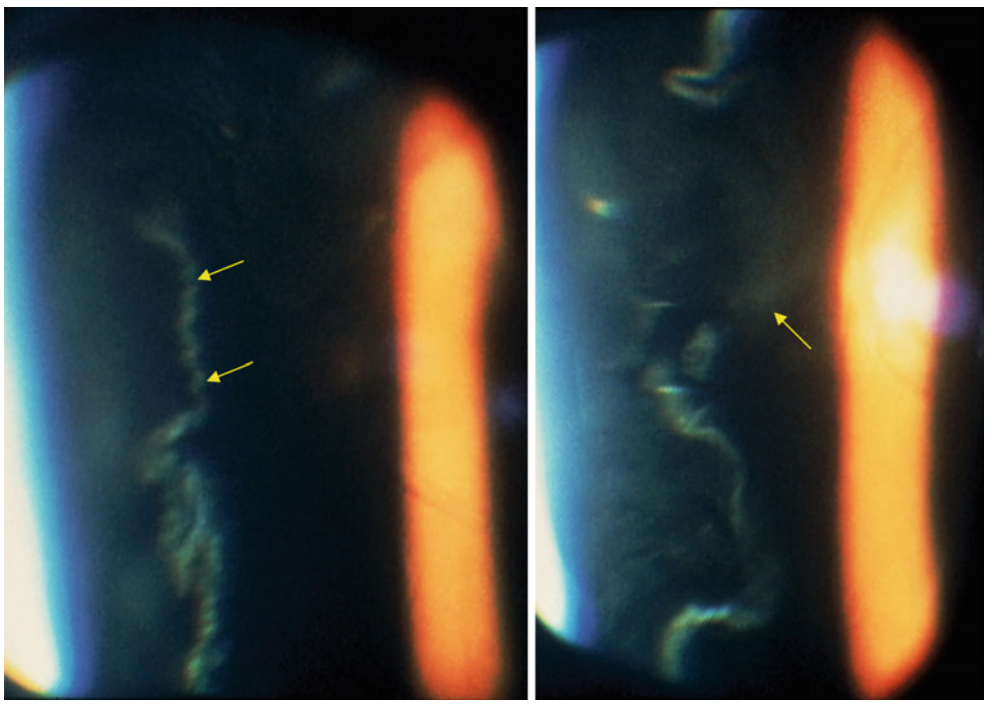

Fig. 11.10 Slit-lamp biomicroscopy of posterior vitreous detachment. (*Left*) posterior vitreous cortex (*yellow arrows*) is seen anterior to the macula. (*Right*) vitreous gel (*yellow arrow*) extruded posteriorly through the premacular defect of the vitreous cortex

vitreous cortex or posterior wall of PPVP tends to develop trampoline-like detachment. Tangential contraction of the premacular cortex may generate anterior vector which promotes trampoline-like PVD. Strong vitreous retinal adhesion at fovea may modify trampoline to perifoveal PVD. In our prospective study in normal non-myopic eyes (Fig. 11.6) [27], PVD first occurs in paramacular area (stage 1) and progresses to a perifoveal PVD (stage 2). Then vitreous cortex detaches at the fovea (stage 3). In vitreo-foveal separation (stage 3), some individuals may have an intact cortex and some may have a break in the cortex. Finally vitreous detachment at the disc results in

Fig. 11.11 Weiss ring in detached vitreous cortex

complete PVD with Weiss ring (stage 4). Figure 11.12 shows the incidence of each stage in different decades in normal non-myopic population [27].

11.3.4 Splitting of Vitreous Cortex

Because of lamellar structure of the vitreous cortex, splitting of vitreous cortex may occur especially at the posterior wall of the PPVP. In our study of normal human eyes with spectral domain OCT [20], splitting of the vitreous cortex was seen in 22 % of the eyes aged over 51 years (Fig. 11.13). In case of persistent vitreous traction such as vitreomacular traction syndrome, vitreous cortex splitting is more likely to occur [37] (Fig. 11.14). This suggests the possibility that outer layer of vitreous cortex may remain on the retina after PVD even with detachment of intact posterior wall of the PPVP. Sebag called the splitting of vitreous cortex as "vitreoschisis" and formed a basis to explain vitreoretinal interface diseases [12, 38].

11.4 Vitreous Changes in Myopic Eyes

11.4.1 Formation of Large Lacuna

Axial myopia is associated with vitreous liquefaction and PVD occurring at a younger age as compared to non-myopic eyes [39–41]. High myopic eyes have a large liquefied lacuna which may mimic PVD (Fig. 11.9 right). Because liquefied vitreous is a source of subretinal fluid in rhegmatogenous retinal detachment without PVD, retinal detachment is more likely to develop in myopic eyes. During PVD a large amount of liquefied vitreous escapes to retrohyaloid space resulting in vitreous collapse. Retinal detachment tends to be severe in high myopic eyes.

It is not well understood why highly myopic eyes develop a large lacuna. In chick model of form-deprivation myopia, axial elongation is associated with an elongation of the vitreous chamber depth and an increase of the vitreous volume [42, 43]. An increase in the vitreous in myopic eyes was attributed on changes in the volume of the liquid vitreous, but not of the gel vitreous [42]. Using this chick model, Seko et al. found the disturbance of electrolyte balance in the vitreous [44]. The concentration of potassium and phosphate were decreased in liquefied vitreous, whereas chloride was increased. Potassium is released from the retina into the vitreous to maintain the homeostatic condition of the retina, and Müller cell plays an important role to regulate the extracellular potassium [45]. Visual deprivation may cause reduction of phototransduction and metabolic activity in the retina, particularly Müller cells. Since the vitreous gel seems to be generated from retina or Müller cells, reduced metabolic activity of the retina or Müller cell in axial myopia may cause formation of large lacuna.

OCT reveals that posterior aspect of PPVP is preserved despite the vitreous liquefaction. Liquefied lacuna may be formed early in central part of the vitreous. In such case, PPVP maintains normal configuration with sharply demarcated anterior border. Liquefied lacuna presents anterior to PPVP with intervening vitreous gel (Fig. 11.15). There is a significant correlation between the PPVP height and myopic refractive error [22]. In myopic eye, PPVP is enlarged and its anterior border becomes irregular. Even though, the posterior wall of PPVP and the septum adjacent to Cloquet's canal are preserved (Fig. 11.16). In case of large PPVP, perifoveal PVD may occur at a young age (Figs. 11.16 and 11.17). If PPVP is markedly large, its anterior border is out of the scope of SS-OCT (Figs. 11.17 and 11.18). Even in such condition, posterior wall of PPVP and the connecting channel are preserved and perifoveal PVD is common (Figs. 11.16, 11.17, and 11.18). The configuration of the PPVP is almost symmetrical in both eyes of each subject. However, if refractive error differs in both eyes of the subject, the configuration and size of PPVP differs in both eyes (Fig. 11.19).

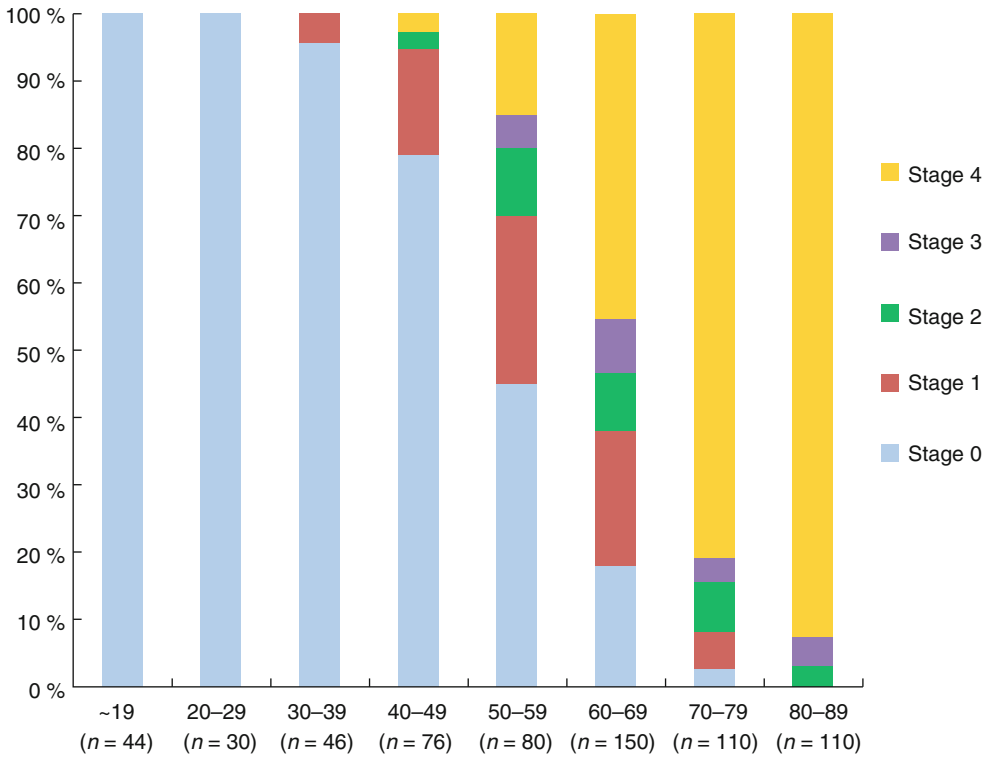

Fig. 11.12 The incidence of each stage in different decades in normal non-myopic population. Stage 4 is complete PVD and stage 0 is no PVD (Reproduced from Itakura and Kishi [27])

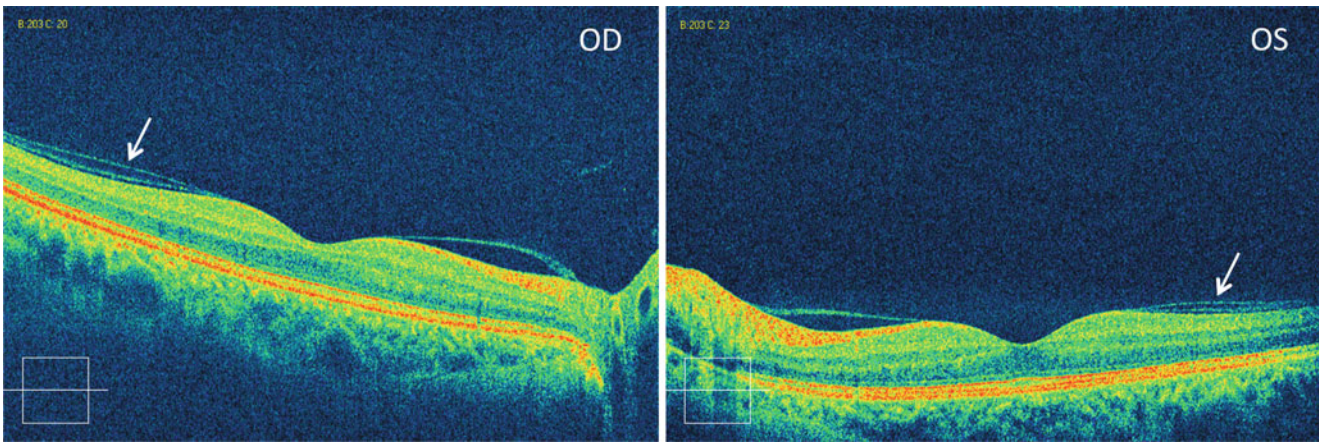

Fig. 11.13 Splitting of vitreous cortex (*arrow*) in both eyes of a 58-year-old female. Horizontal sections of SD-OCT (Reprint from Itakura and Kishi [20])

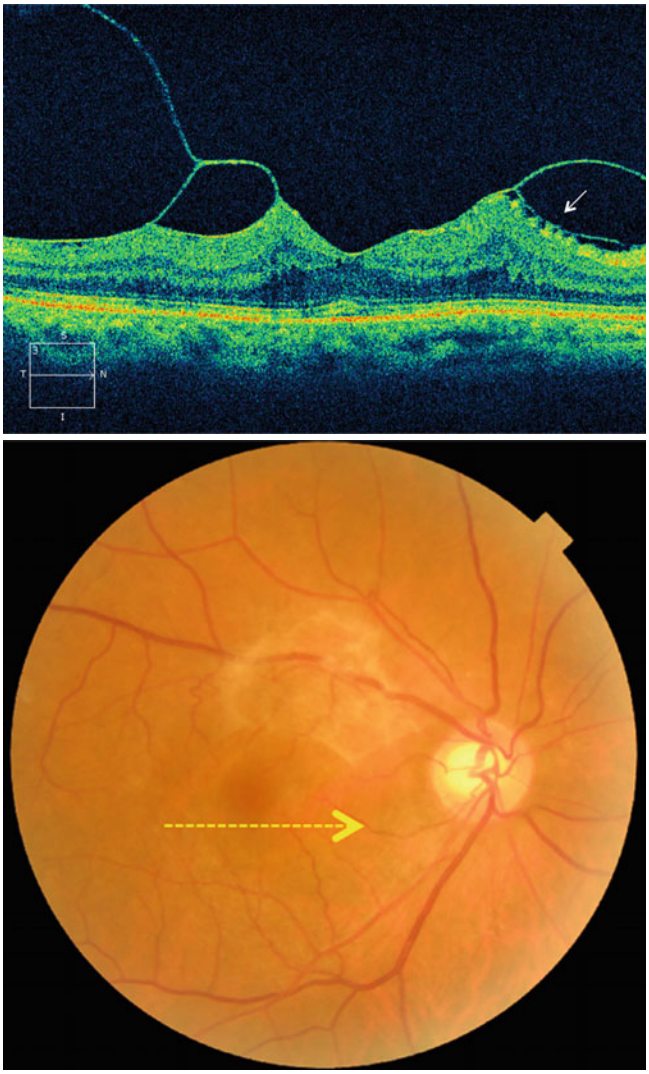

Fig. 11.14 Vitreous cortex splitting (*arrow*) in vitreomacular traction syndrome (Reprint from Itakura and Kishi [37])

11.4.2 Incomplete PVD

The features of incomplete PVD in high myopia were first demonstrated by SS-OCT. If Weiss ring is not detected despite anterior displacement of vitreous gel by slit-lamp biomicroscopy, we should consider it a large PPVP or extensive liquefaction. SS-OCT can better detect the vitreous cortex or posterior wall of PPVP attached on the retina or partially detached. Perifoveal PVD is common in myopic eyes as in non-myopic eyes. In case of no PVD on slit-lamp biomicroscopy, SS-OCT well visualized the posterior vitreous cortex detached at the macula, but attached to optic disc (Fig. 11.20 top). In case of vitreomacular separation, posterior wall of the PPVP may attach on the retina which acts as epiretinal membrane (Fig. 11.20 bottom). SS-OCT demonstrates the flatten PPVP in case of PVD in the macular area (Fig. 11.21). PPVP may have an intact posterior wall or a disrupted wall (Fig. 11.6 bottom).

11.4.3 Early PVD

We prospectively investigated the posterior vitreous using SD-OCT or SS-OCT in non-myopic eyes (control) and high myopia of more than −8.0D. We defined complete PVD as detached vitreous cortex with Weiss ring. In ages from 20 to 39 years, control eyes had only 8.3 % partial PVD, while high myopic eyes had already 27.8 % of complete PVD and 16.7 % of partial PVD (Fig. 11.22). In the ages of 40–59 years, high myopics had 43.2 % of complete PVD and 35.1 % of partial PVD, while control eyes had only 8.2 % of complete PVD and 38.8 % of partial PVD (Fig. 11.23). In ages between 60 and 79 years, high myopics had 91.4 % of complete PVD and 8.6 % of partial PVD, while control eyes had 60.6 % of complete PVD and 29.4 % of partial PVD (Fig. 11.24).

11.4.4 Residual Vitreous Cortex in Eyes with Complete PVD

Residual vitreous cortex attached on the retina is only detected by SS-OCT. In our prospective study, residual cortex was seen in 6.7 % of 105 non-myopic eyes with PVD and 37.7 % of 53 highly myopic eyes (Fig. 11.25).

It is difficult to evaluate the vitreous by slit-lamp biomicroscopy in myopic eyes. If we observe anterior displacement of vitreous gel with extensive liquefaction but no Weiss ring, we assume no PVD. SS-OCT gives more concrete answer demonstrating the posterior wall of the PPVP and the septum adjacent to Martegiani space (Fig. 11.26 top). Vitreous surgeons frequently note the residual vitreous cortex in posterior staphyloma despite the apparent PVD with Weiss ring during surgery in myopic foveoschisis eyes. SS-OCT demonstrates the residual vitreous cortex in the eyes of myopic foveoschisis with PVD with Weiss ring (Fig. 11.26 bottom).

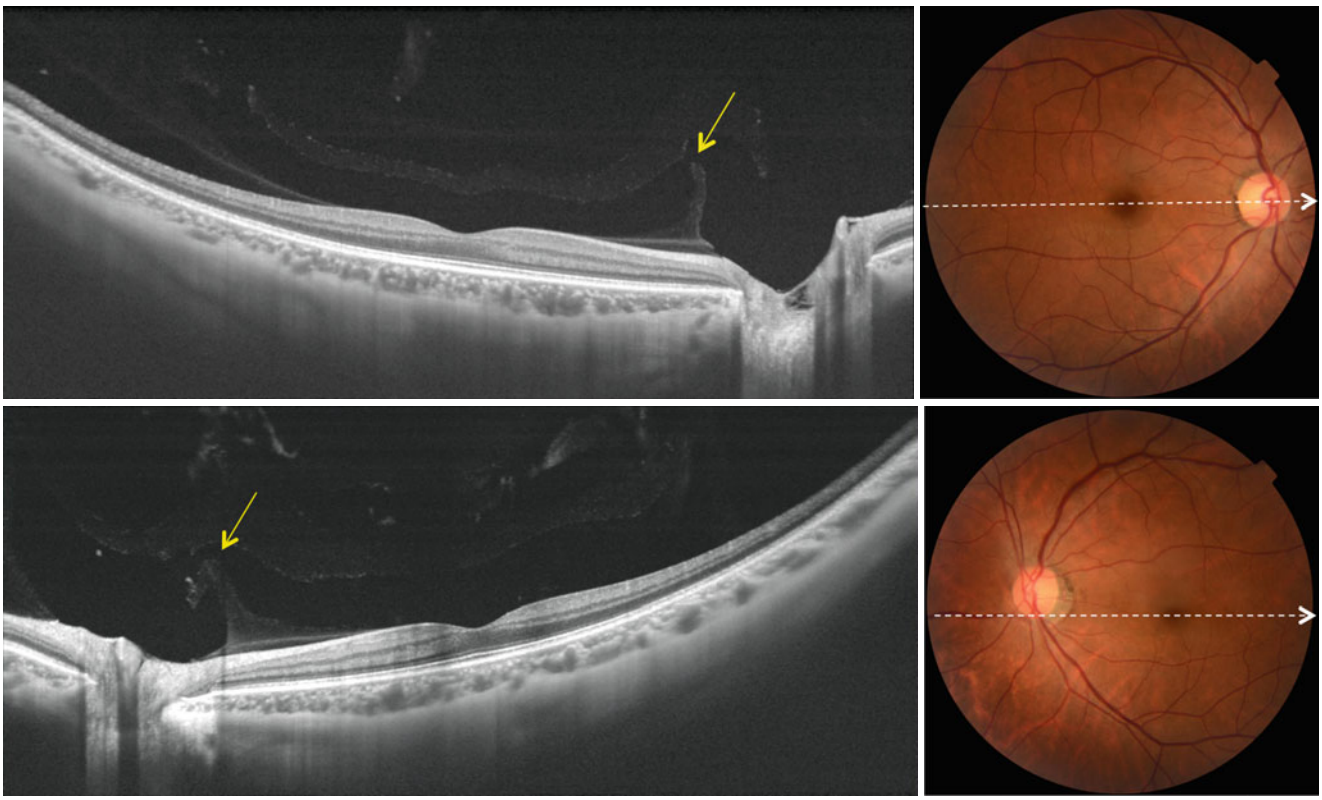

Fig. 11.15 A 46-year-old female. Her vision was 1.2×−5.5D in the right and 1.2×−8.5D in the left eye. There is a similarity in the configuration of posterior precortical vitreous pocket (PPVP) in both eyes. PPVP is a flat boat shaped. Connecting channel (*arrow*) between PPVP and Martegiani space of Cloquet's canal. There are liquefied spaces superior to the PPVP in both eyes

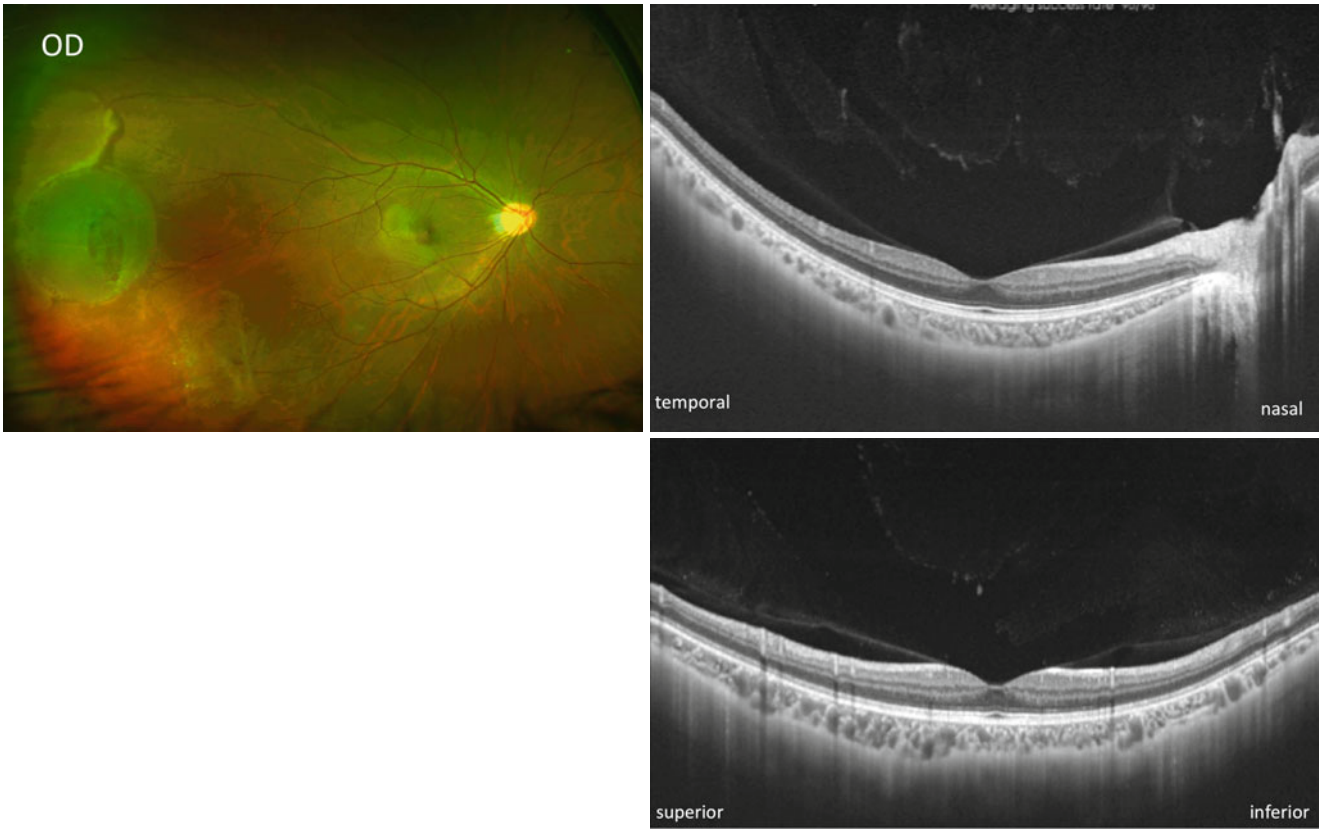

Fig. 11.16 Right eye of a 24-year-old male with moderate myopia. He had focal retinal detachment in the temporal periphery of the right eye. His vision was 1.2×−5.0D in the right and 1.2×−5.5D in the left eye. No PVD was noted biomicroscopically in the right eye. SS-OCT showed relatively large posterior precortical vitreous pocket (PPVP) with irregular anterior border. Perifoveal PVD is noted in horizontal (*right top*) and vertical (*right bottom*) sections. Septum between PPVP and Martegiani space of Cloquet's canal is seen in the horizontal section

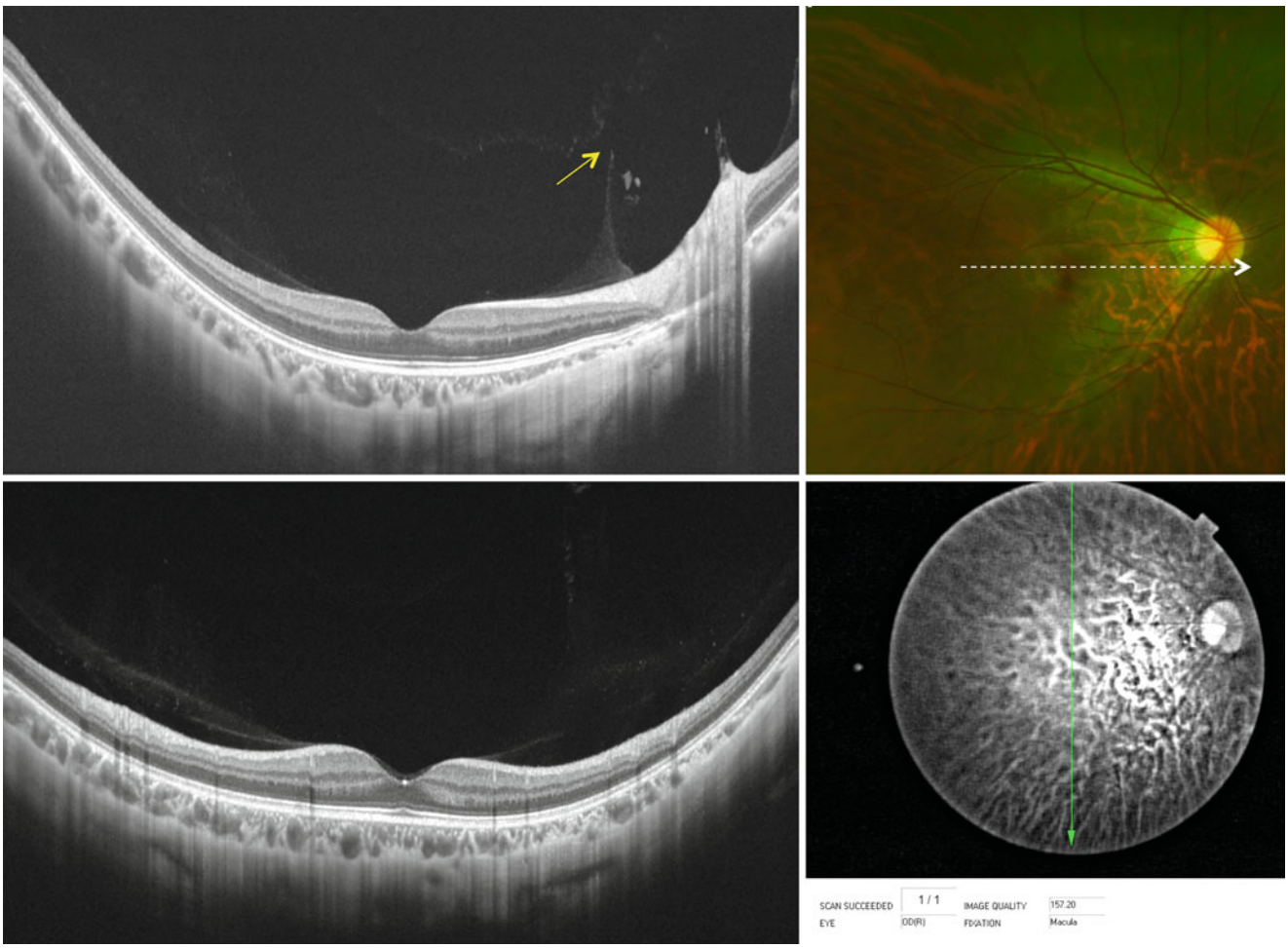

Fig. 11.17 A 21-year-old male. His vision was 1.2×−11.0D in the right eye which showed liquefaction but no PVD in slit-lamp biomicroscopy. His fellow eye underwent retinal detachment surgery. *Top*: SS-OCT shows large posterior precortical vitreous pocket (PPVP); the connecting channel (*arrow*) is seen at the top of the septum. *Bottom*: large PPVP and perifoveal PVD is seen

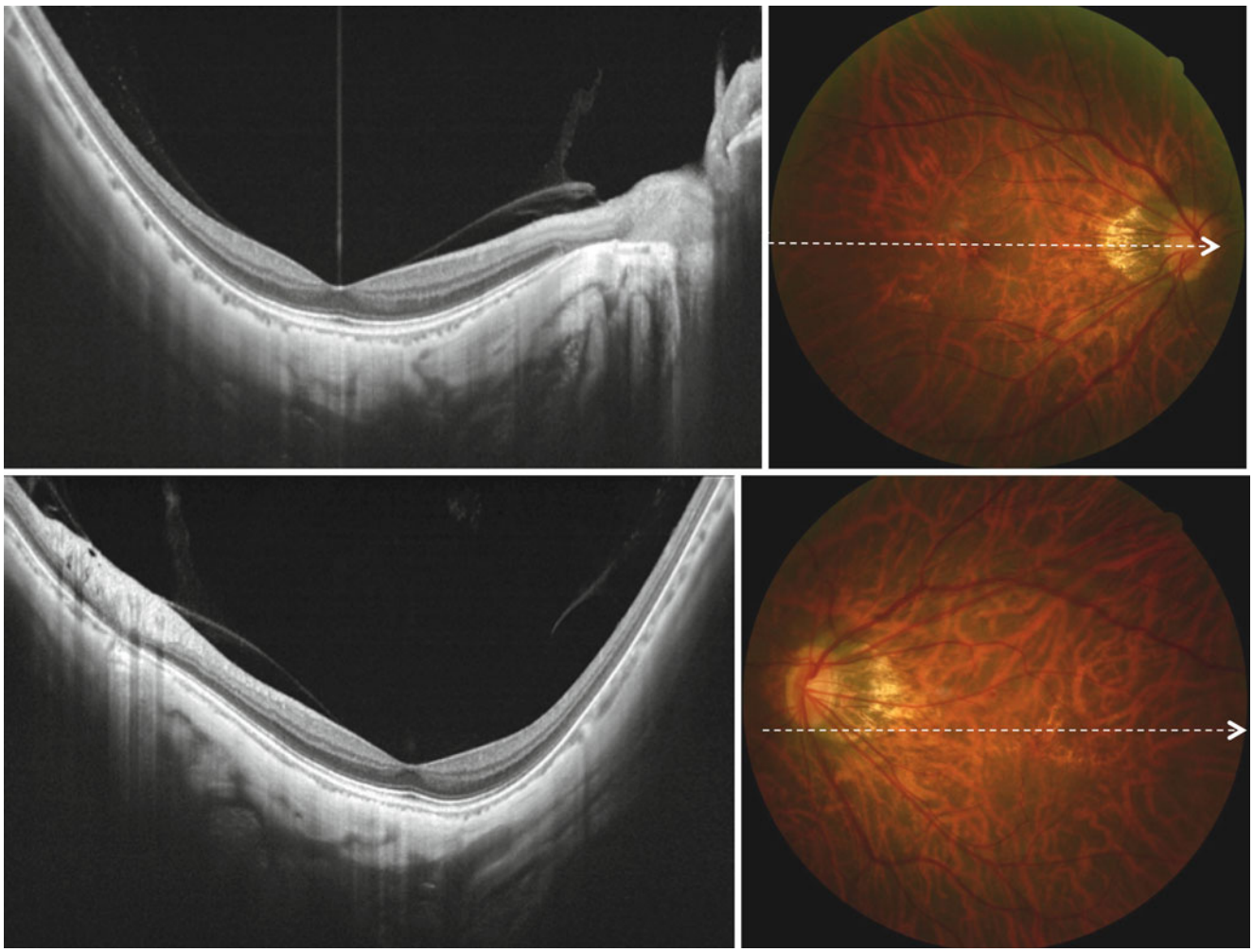

Fig. 11.18 A 48-year-old female. Her vision was 1.2×−11.5D in the right and 1.2×−12.5D. Both eyes had large posterior precortical vitreous pocket whose anterior border was not detected. Focal PVD was seen in paramacular area in both eyes

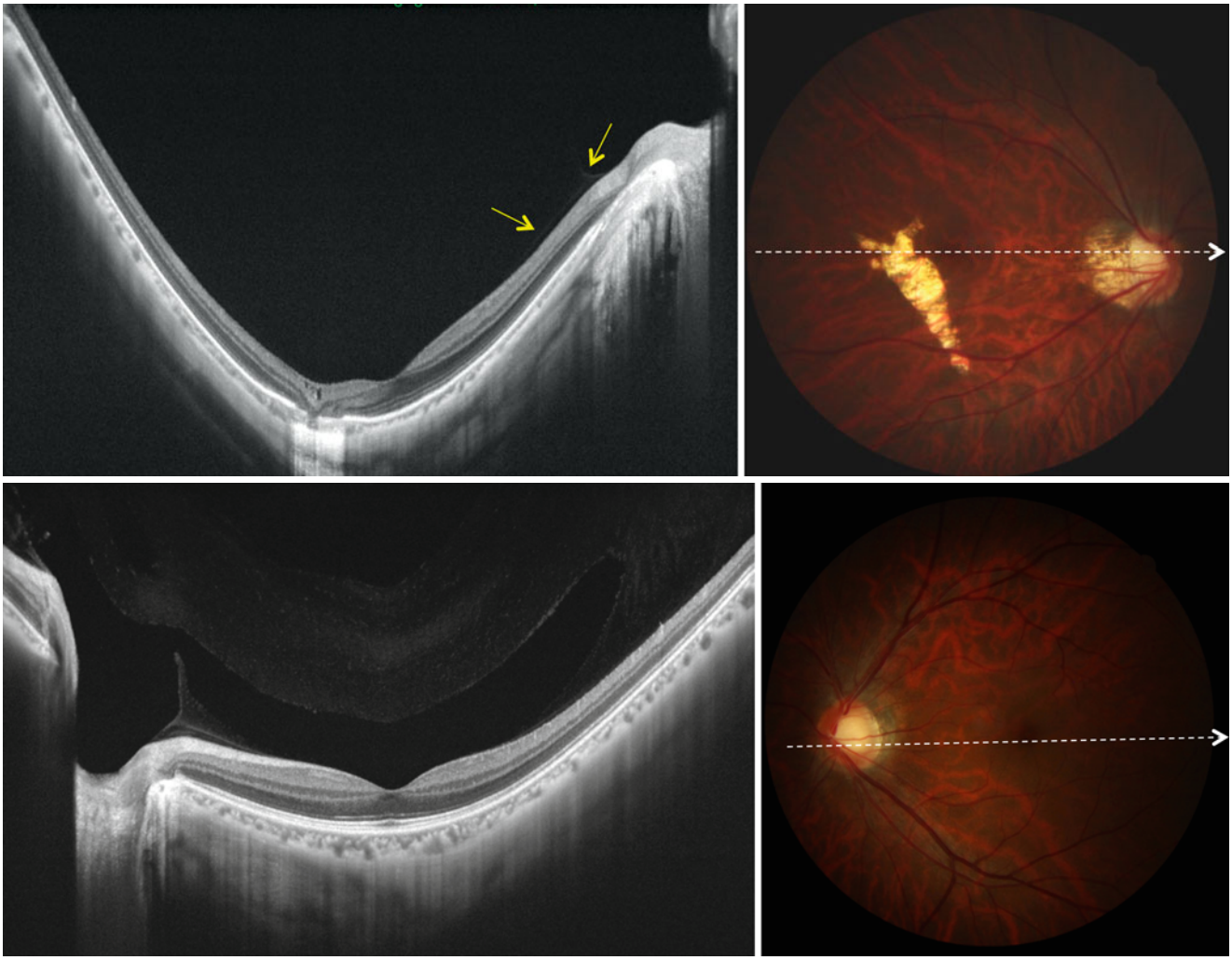

Fig. 11.19 A 44-year-old man with enlarged lacquer crack in his right eye. His vision is 1.0×−12.0D in the right and 1.2×−6.0D in the left eye. No PVD was detected in both eyes. *Top*: SS-OCT showed extensive liquefaction, and anterior border of posterior precortical vitreous pocket (PPVP) was not detected in the right eye. Slightly detached vitreous cortex and the septum at temporal border of Cloquet's canal were seen (*arrows*). *Bottom*: the left eye showed boat-shaped PPVP. There is a liquefied lacuna anterior to the PPVP

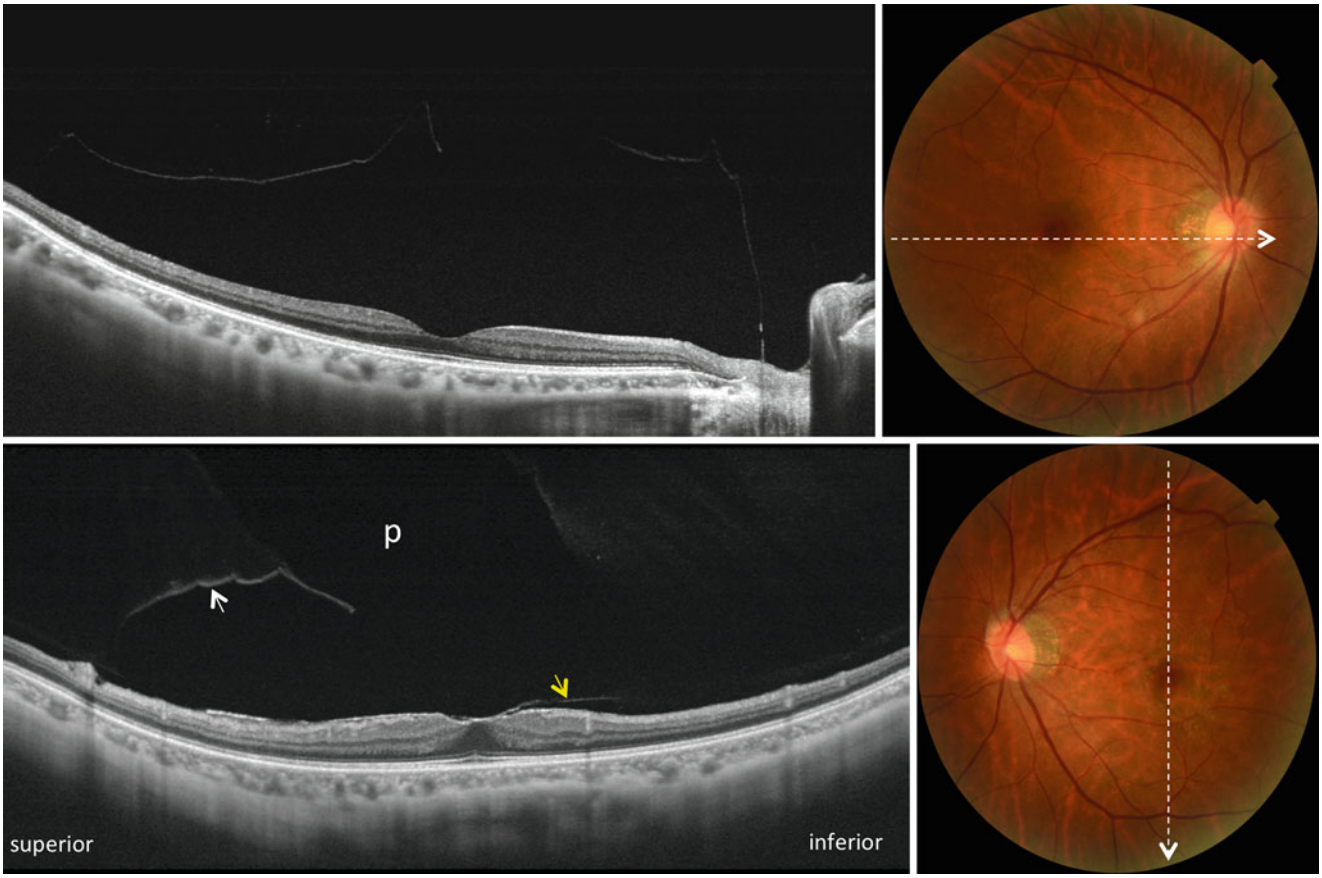

Fig. 11.20 A 59-year-old woman with epiretinal membrane in the left eye. Her vision was 1.2×−10D in the right and 1.2×−7.0D in the left eye. *Top*: the right eye had PVD in the macular area but vitreous cortex attached to the optic disc. The detached posterior wall of the posterior precortical vitreous pocket (PPVP) which is a premacular vitreous cortex was disrupted. *Bottom*: in the vertical section of the left eye, vitreous cortex was detached in the superior to the fovea (*white arrow*), but attached on the inferior to the fovea. Epiretinal membrane (*yellow arrow*) appears to correspond to the posterior wall of the PPVP which is seen as an empty space (*p*)

Fig. 11.21 A 43-year-old female. Her vision is 1.2×−6.0D in the right eye. SS-OCT showed PVD in the macular area but vitreous attached at optic disc. Premacular vitreous cortex which is a posterior wall of the posterior precortical vitreous pocket (PPVP) was intact (*top* and *bottom*). There is a connecting channel (*arrow*) between PPVP and Martegiani space of Cloquet's canal in horizontal section (*top*). Her left eye had retinal detachment

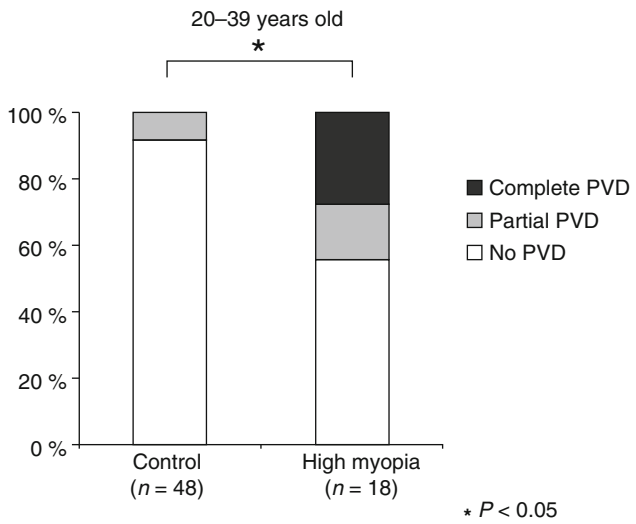

Fig. 11.22 The incidence of PVD in non-myopic control and high myopia of more than −8.0D in the population of 20–39 years old

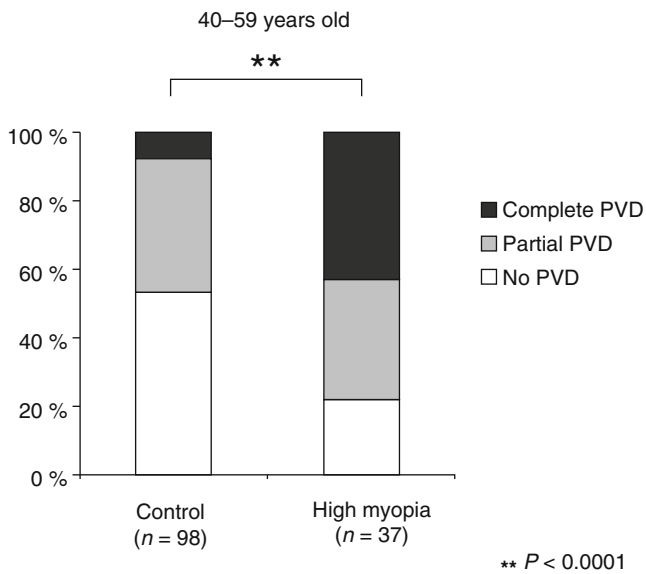

Fig. 11.23 The incidence of PVD in non-myopic control and high myopia of more than −8.0D in the population of 40–59 years old

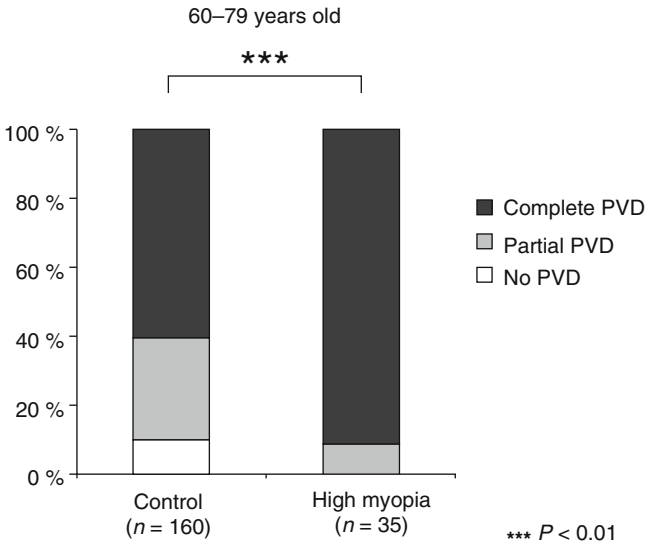

Fig. 11.24 The incidence of PVD in non-myopic control and high myopia of more than −8.0D in the population of 60–79 years old

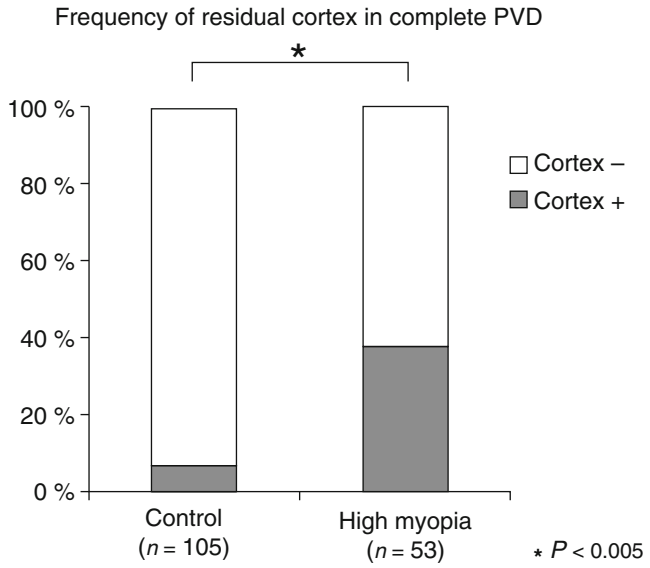

Fig. 11.25 Frequency of residual cortex with complete PVD detected by SS-OCT in non-myopic control and high myopia more than −8.0D

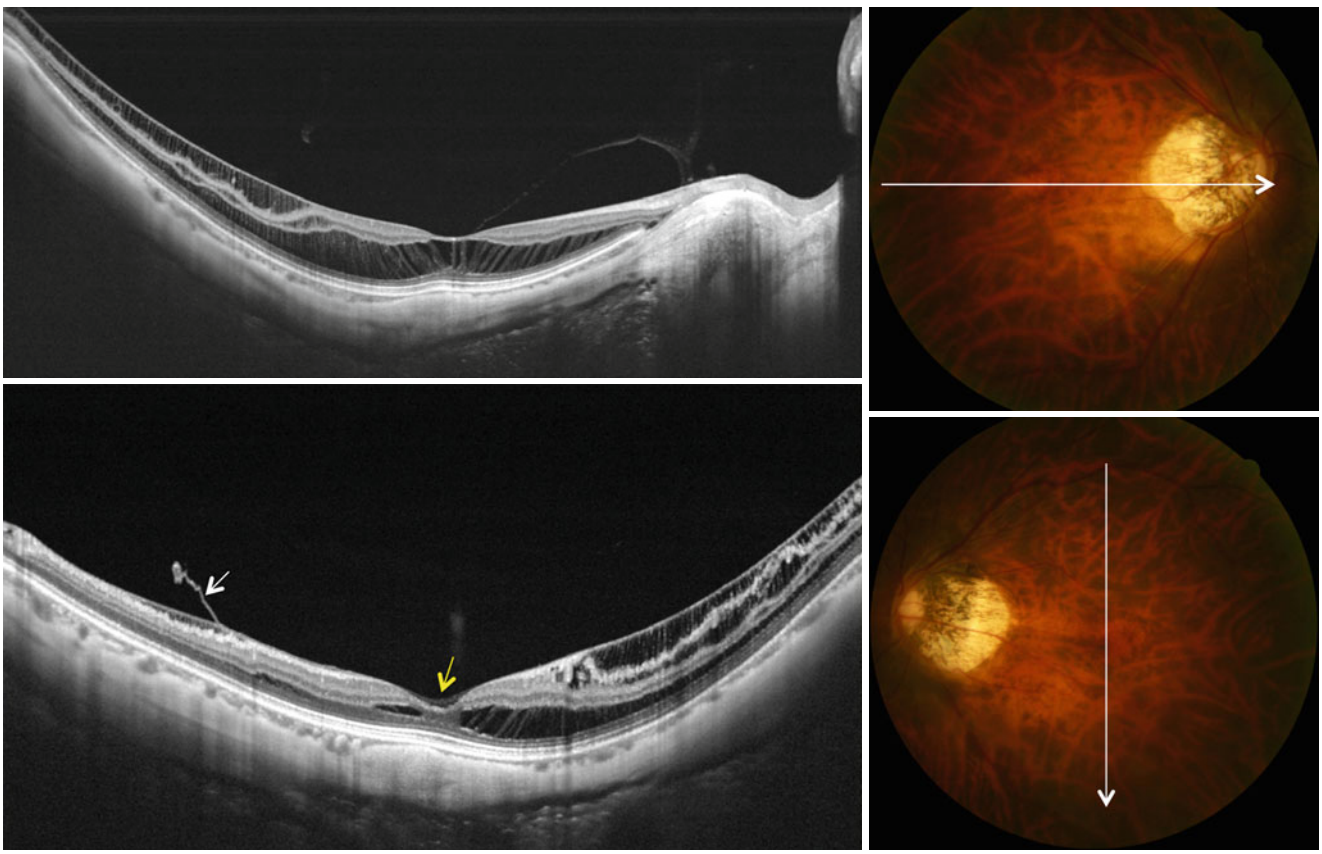

Fig. 11.26 A 58-year-old woman has myopic foveoschisis in both eyes. Her vision is 1.2×−14.0D in both eyes. Slit-lamp biomicroscopy showed no PVD in the right and PVD with Weiss ring in the left eye. *Top*: SS-OCT showed partially detached vitreous cortex nasal to the fovea in the right eye. Anterior border of PPVP is not seen. *Bottom*: partially detached epiretinal membrane (*white arrow*) is seen superior to the fovea, from which the membrane attached on the retina to the fovea (*yellow arrow*)

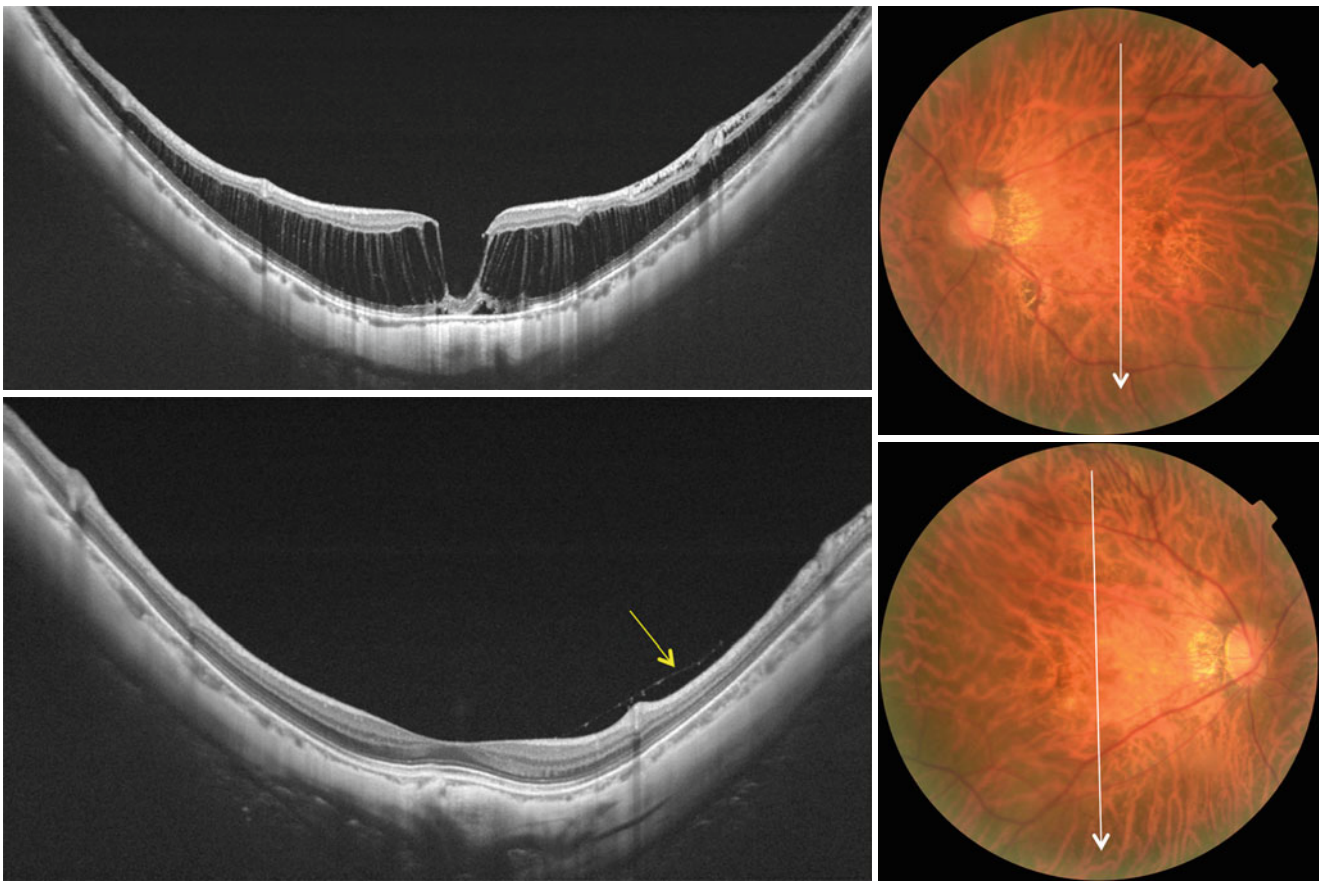

Fig. 11.27 A 70-year-old female with myopic foveoschisis in the right eye. Her vision was 0.8p×−10.5D in the right and 1.2×−9.0D in the left eye. Both eyes had PVD with Weiss ring. There was no residual vitreous cortex on the retina in the right eye (*top*), which was later confirmed by vitrectomy for foveoschisis. There is a slightly detached vitreous cortex (*arrow*) inferior to the macula in the left eye despite PVD (*bottom*)

During vitreous surgery for myopic foveoschisis with complete PVD, we occasionally encounter the case with no residual vitreous cortex. In such case, we only remove ILM in the posterior pole. SS-OCT clearly demonstrates no vitreous cortex on the retina preoperatively (Fig. 11.27 top). Despite the apparent PVD with Weiss ring, very thin vitreous cortex may remain on the retina in highly myopic eyes (Figs. 11.27 bottom, and 11.28). The residual cortex can be interpreted as the remnants of posterior wall of PPVP or outermost layer of the split vitreous cortex. It may be not a residual cortex but a newly formed epiretinal membrane by proliferated glial cells or pigment epithelial cells. Another possibility is regenerated vitreous cortex after PVD which yet to be proved.

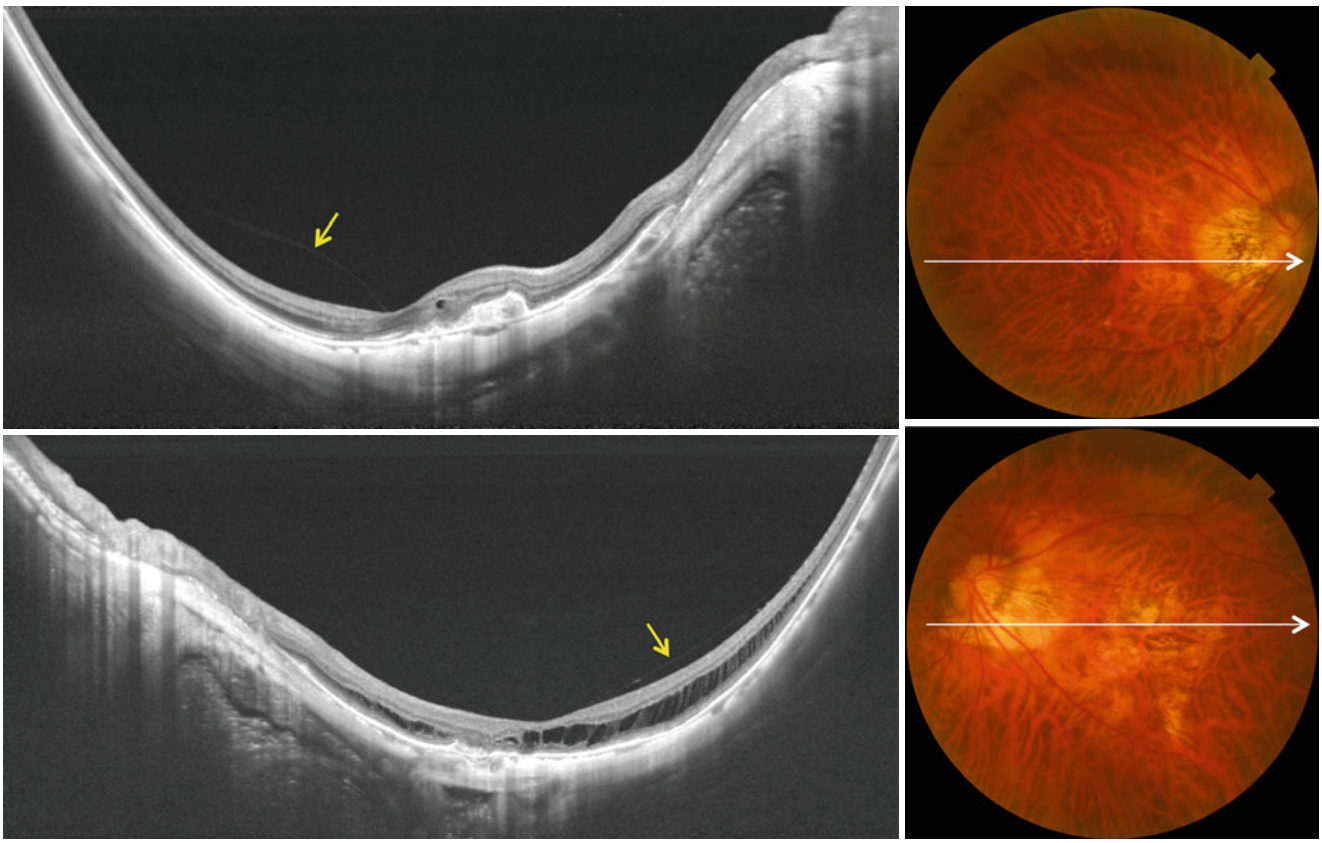

Fig. 11.28 A 73-year-old woman. She has myopic choroidal neovascularization which was treated by intravitreal bevacizumab in the right eye. The left eye has myopic foveoschisis. Her vision is 0.5×−15.0D in the right and 0.1×−15.0D in the left eye. Although PVD with Weiss ring was observed in both eyes on slit-lamp biomicroscopy, SS-OCT revealed slightly detached thin possibly vitreous cortex (*arrow*) temporal to the fovea in both eyes (*top* and *bottom*)

Conclusion

The pathological condition of the vitreous in posterior staphyloma has been unclear because of invisible structure by slit-lamp biomicroscopy. Using time-domain OCT, we first reported myopic foveoschisis [1] in 1999. At that time, time-domain OCT could not depict the vitreous structure. Recently developed SS-OCT sheds light on the manifestation of vitreous cortex in high myopia. The posterior wall of PPVP plays an important role in vitreoretinal interface diseases in high myopia as well as in non-myopic eyes.

References

1. Takano M, Kishi S. Foveal retinoschisis and retinal detachment in severely myopic eyes with posterior staphyloma. Am J Ophthalmol. 1999;128(4):472–6.
2. Kobayashi H, Kishi S. Vitreous surgery for highly myopic eyes with foveal detachment and retinoschisis. Ophthalmology. 2003;110(9):1702–7.
3. Schepens CL, Marden D. Data on the natural history of retinal detachment. Further characterization of certain unilateral nontraumatic cases. Am J Ophthalmol. 1966;61(2):213–26.
4. Tolentino FI, Schepens CL, Freeman HM. Vitreoretinal disorders. Philadelphia: W.B. Sanders Co.; 1976. p. 1–12.
5. Eisner G. Biomicroscopy of the peripheral fundus. New York: Springer; 1979. p. 20, 21, 106, 107.
6. Yokoi T, Toriyama N, Yamane T, Nakayama Y, Nishina S, Azuma N. Development of a premacular vitreous pocket. JAMA Ophthalmol. 2013;131(8):1095–6.
7. Kishi S, Shimizu K. Posterior precortical vitreous pocket. Arch Ophthalmol. 1990;108(7):979–82.
8. Schmut O, Mallinger R, Paschke E. Studies on a distinct fraction of bovine vitreous body collagen. Graefes Arch Clin Exp Ophthalmol. 1984;221(6):286–9.
9. Bishop PN, Crossman MV, McLeod D, Ayad S. Extraction and characterization of the tissue forms of collagen types II and IX from bovine vitreous. Biochem J. 1994;299(Pt 2):497–505.
10. Sakamoto T, Ishibashi T. Hyalocytes: essential cells of the vitreous cavity in vitreoretinal pathophysiology? Retina. 2011;31(2):222–8.
11. Ramesh S, Bonshek RE, Bishop PN. Immunolocalisation of opticin in the human eye. Br J Ophthalmol. 2004;88(5):697–702.
12. Gupta P, Yee KM, Garcia P, Rosen RB, Parikh J, Hageman GS, Sadun AA, Sebag J. Vitreoschisis in macular diseases. Br J Ophthalmol. 2011;95(3):376–80.
13. Foos RY. Vitreoretinal juncture; topographical variations. Invest Ophthalmol. 1972;11(10):801–8.
14. Kishi S, Numaga T, Yoneya S, Yamazaki S. Epivascular glia and paravascular holes in normal human retina. Graefes Arch Clin Exp Ophthalmol. 1986;224(2):124–30.

15. Worst JG. Cisternal systems of the fully developed vitreous body in the young adult. Trans Ophthalmol Soc U K. 1977;97(4): 550–4.
16. Worst J. Extracapsular surgery in lens implantation (Binkhorst lecture). Part IV. Some anatomical and pathophysiological implications. J Am Intraocul Implant Soc. 1978;4:7–14.
17. Worst J, Los L. Cisternal anatomy of the vitreous. Amsterdam: Kugler Publications; 1995. p. 28.
18. Sebag J, Balazs EA. Human vitreous fibers and vitreoretinal disease. Trans Ophthalmol Soc U K. 1985;104:123–8.
19. Fine HF, Spaide RF. Visualization of the posterior precortical vitreous pocket in vivo with triamcinolone. Arch Ophthalmol. 2006;124(11):1663.
20. Itakura H, Kishi S. Aging changes of vitreomacular interface. Retina. 2011;31(7):1400–4.
21. Itakura H, Kishi S. Alterations of posterior precortical vitreous pockets with positional changes. Retina. 2013;33(7):1417–20.
22. Itakura H, Kishi S, Li D, Akiyama H. Observation of posterior precortical vitreous pocket using swept-source optical coherence tomography. Invest Ophthalmol Vis Sci. 2013;54(5):3102–7.
23. Balazs EA. The vitreous. In: Zinn K, editor. Ocular fine structure for the clinician, vol. 15. Boston: Little, Brown; 1973. p. 53–63.
24. Kishi S, Hagimura N, Shimizu K. The role of the premacular liquefied pocket and premacular vitreous cortex in idiopathic macular hole development. Am J Ophthalmol. 1996;122(5):622–8.
25. Johnson MW, Van Newkirk MR, Meyer KA. Perifoveal vitreous detachment is the primary pathogenic event in idiopathic macular hole formation. Arch Ophthalmol. 2001;119(2):215–22.
26. Uchino E, Uemura A, Ohba N. Initial stages of posterior vitreous detachment in healthy eyes of older persons evaluated by optical coherence tomography. Arch Ophthalmol. 2001;119(10): 1475–9.
27. Itakura H, Kishi S. Evolution of vitreomacular detachment in healthy subjects. Arch Ophthalmol. 2013: 4578 doi: 10.1001/jamaophthalmol.2013.4578. [Epub ahead of print].
28. Kishi S, Demaria C, Shimizu K. Vitreous cortex remnants at the fovea after spontaneous vitreous detachment. Int Ophthalmol. 1986;9(4):253–60.
29. Kishi S, Shimizu K. Oval defect in detached posterior hyaloid membrane in idiopathic preretinal macular fibrosis. Am J Ophthalmol. 1994;118(4):451–6.
30. Kishi S, Shimizu K. Clinical manifestations of posterior precortical vitreous pocket in proliferative diabetic retinopathy. Ophthalmology. 1993;100(2):225–9.
31. Imai M, Iijima H, Hanada N. Optical coherence tomography of tractional macular elevations in eyes with proliferative diabetic retinopathy. Am J Ophthalmol. 2001;132:81–4.
32. Spaide RF, Wong D, Fisher Y, Goldbaum M. Correlation of vitreous attachment and foveal deformation in early macular hole states. Am J Ophthalmol. 2002;133(2):226–9.
33. Balazs EA, Flood MT. Data first presented at 3rd International Congress for Eye Research, Osaka, Japan. In: Sebag J, editor. The vitreous. New York: Springer; 1989. p. 81.
34. Foos RY, Wheeler NC. Vitreoretinal juncture. Synchysis senilis and posterior vitreous detachment. Ophthalmology. 1982;89(12): 1502–12.
35. Sebag J. The vitreous. New York: Springer; 1989. p. 41, 76, 78, 79, 85.
36. Itakura H, Kishi S, Kotajima N, Murakami M. Decreased vitreal hyaluronan levels with aging. Ophthalmologica. 2009; 223(1):32–5.
37. Itakura H, Kishi S. Vitreous cortex splitting in cases of vitreomacular traction syndrome. Ophthalmic Surg Lasers Imaging. 2012;43 Online:e27–9.
38. Sebag J. Anomalous posterior vitreous detachment: a unifying concept in vitreo-retinal disease. Graefes Arch Clin Exp Ophthalmol. 2004;242(8):690–8.
39. Sanna G, Nervi I. Statistical research on vitreal changes in relation to age and refraction defects]. Ann Ottalmol Clin Ocul. 1965; 91(5):322–35.
40. Novak MA, Welch RB. Complications of acute symptomatic posterior vitreous detachment. Am J Ophthalmol. 1984;97(3):308–14.
41. Akiba J. Prevalence of posterior vitreous detachment in high myopia. Ophthalmology. 1993;100(9):1384–8.
42. Pickett-Seltner RL, Doughty MJ, Pasternak JJ, Sivak JG. Proteins of the vitreous humor during experimentally induced myopia. Invest Ophthalmol Vis Sci. 1992;33(12):3424–9.
43. Wallman J, Adams JI. Developmental aspects of experimental myopia in chicks: susceptibility, recovery and relation to emmetropization. Vision Res. 1987;27(7):1139–63.
44. Seko Y, Shimokawa H, Pang J, Tokoro T. Disturbance of electrolyte balance in vitreous of chicks with form-deprivation myopia. Jpn J Ophthalmol. 2000;44(1):15–9.
45. Newman EA. Regional specialization of retinal glial cell membrane. Nature. 1984;309(5964):155–7.
46. Jongebloed WL, Worst JF. The cisternal anatomy of the vitreous body. Doc Ophthalmol. 1987;67(1–2):183–96.